Fuzzy Adaptive Constrained Consensus Tracking of High-Order Multi-agent Networks
A New Event-Triggered Mechanism

Wang, Ning; Wang, Ying; Wen, Guanghui; Lv, Maolong; Zhang, Fan

DOI
10.1109/TSMC.2021.3127825

Publication date
2022

Document Version
Final published version

Published in
IEEE Transactions on Systems, Man, and Cybernetics: Systems

Citation (APA)
Wang, N., Wang, Y., Wen, G., Lv, M., & Zhang, F. (2022). Fuzzy Adaptive Constrained Consensus Tracking of High-Order Multi-agent Networks: A New Event-Triggered Mechanism. *IEEE Transactions on Systems, Man, and Cybernetics: Systems*, *52*(9), 5468-5480. https://doi.org/10.1109/TSMC.2021.3127825

Fuzzy Adaptive Constrained Consensus Tracking of High-Order Multi-Agent Networks: A New Event-Triggered Mechanism

Ning Wang, Ying Wang, Guanghui Wen, *Senior Member, IEEE*, Maolong Lv, and Fan Zhang

***Abstract*—This article aims to realize event-triggered constrained consensus tracking for high-order nonlinear multiagent networks subject to full-state constraints. The main challenge of achieving such goals lies in the fact that the standard designs [e.g., backstepping, event-triggered control, and barrier Lyapunov functions (BLFs)] successfully developed for low-order dynamics fail to work for high-order dynamics. To tackle these issues, a novel high-order event-triggered mechanism is devised to update the actual control input, lowering the communication and computation burden. More precisely, compared with the conventional event-triggered mechanism, not only the amplitudes of control signals and a fixed threshold are considered but a monotonically decreasing function is introduced to allow a relatively big threshold, while guaranteeing consensus tracking error to be small. Then, a high-order tan-type BLF working for both constrained and unconstrained scenarios is incorporated into the distributed adding-one-power-integrator design for the purpose of confining full states within some compact sets all the time. A finite-time convergent differentiator (FTCD) is introduced to circumvent the "explosion of complexity." The consensus tracking error is shown to eventually converge to a residual set whose size can be adjusted as small as desired through choosing appropriate design parameters. Comparative simulations have been conducted to highlight the superiorities of the developed scheme.**

***Index Terms*—Event-triggered control (ETC), full-state constraints, high-order multiagent networks.**

Manuscript received 5 February 2021; revised 19 May 2021 and 20 September 2021; accepted 1 November 2021. Date of publication 30 November 2021; date of current version 18 August 2022. This work was supported in part by the National Key Research and Development Program of China under Project 2020YFC2200800 and Project 2020YFC2200801; in part by the National Natural Science Foundation of China under Grant 61703099, Grant 62073079, and Grant 62088101; and in part by the State Key Laboratory of Intelligent Control and Decision of Complex Systems, Beijing Institute of Technology. This article was recommended by Associate Editor W. Sun. *(Corresponding author: Guanghui Wen.)*

Ning Wang and Ying Wang are with the Air Traffic Control and Navigation College, Air Force Engineering University, Xi'an 710051, Shaanxi, China (e-mail: ning_wang0428@163.com; yingwang_kgd@163.com).

Guanghui Wen is with the Department of Systems Science, School of Mathematics, Southeast University, Nanjing 210096, China (e-mail: wenguanghui@gmail.com).

Maolong Lv is with the Air Traffic Control and Navigation College, Air Force Engineering University, Xi'an 710051, Shaanxi, China, and also with the Delft Center for Systems and Control, Delft University of Technology, 2628 CD Delft, The Netherlands (e-mail: m.lyu@tudelft.nl).

Fan Zhang is with the School of Aeronautics and Astronautics (Shenzhen), Sun Yat-sen University, Guangzhou 510275, China (e-mail: zhangfan6@mail.sysu.edu.cn).

Color versions of one or more figures in this article are available at https://doi.org/10.1109/TSMC.2021.3127825.

Digital Object Identifier 10.1109/TSMC.2021.3127825

I. Introduction

Recent years have witnessed a tremendous progress in the field of distributed control of nonlinear multiagent networks and, in general, they can be classified by two categories: 1) strict-feedback multiagent networks [1]–[3] and 2) pure-feedback multiagent networks [4]–[6], i.e., systems whose dynamics are described or can be transformed into a chain of integrators with power equal to one. For these results, the commonly adopted approach is an extension of the well-known backstepping technique [7] in a distributed sense by introducing one linear integrator at each iteration, and also combined with universal approximators [e.g., fuzzy logic systems (FLSs) and neural networks (NNs)] to handle unparameterized nonlinearities [8]–[10]. Compared to NNs, FLSs are particularly studied since the experience from expert human operators can be systematically included into fuzzy IF-THEN rules to be part of the control [11], [12]. High-order nonlinear multiagent networks are a generalization of strict-feedback or pure-feedback multiagent networks, in which the virtual and actual control terms are the power functions with positive odd integers rather than linear ones. It is well documented in literature that high-order dynamics, appearing in aerospace and robotic applications [13], [14], are extremely challenging to deal with, as their linearized dynamics might possess uncontrollable modes whose eigenvalues are on the right half-plane [15], making all standard feedback linearization or standard backstepping methodologies [1]–[10] inapplicable. The adding-one-power-integrator procedure was therefore proposed in [16] to overcome the aforementioned challenges by introducing one high-power integrator instead of a linear one at each iteration. Since then, fruitful results have been obtained for single high-order system [17]–[19] and multiple high-order systems [20]–[22]. However, it has to be stressed that the above-mentioned results in [17]–[22] suffer from two major drawbacks: 1) they relied on the periodic sampling mechanism and 2) they did not take into account full-state constraints. The importance of those two points are highlighted hereafter.

It is well recognized that the task of the periodic sampling mechanism is to execute every fixed period of time, resulting in unnecessary waste of communication and computing resources [23]. To solve this issue, event-triggered control (ETC) was formulated in [24] where the task is to execute only when the triggering errors are larger than some prespecified thresholds. Since then, massive ETC strategies have been proposed for single systems [25]–[27] and multiagent networks [28]–[32]. Unfortunately, all abovementioned ETC protocols are solely suitable for low-order dynamics (i.e., the powers are equal to one) and cannot be directly applied to high-order cases. This is because the existing event-triggered mechanisms rely on the precondition that the signs of the combination terms of the local tracking errors and the transition control signals are less than or equal to 0. However, the combination terms cannot be obtained and their signs cannot also be determined due to the existence of high powers (see discussions in Remark 6). In addition, the existing thresholds in [23]–[28] and [30]–[32] are composed by the amplitudes of control signals as well as a fixed threshold. Such designs theoretically imply that tracking accuracy is weakened when the magnitudes of control signals become large. In practical scenarios, it usually requires small consensus tracking error, while guaranteeing larger threshold (see discussions in Remark 7). To the best of our knowledge, such an answer is missing in the existing literature. In other words, how to establish a balance between tracking performance and the magnitudes of control signals needs to be further researched. Thence, a new event-triggered mechanism must be sought going beyond the state-of-the-art for high-order multiagent networks.

Besides, in practical engineering systems, the states are typically required to satisfy various restrictions and the violation of these constraints may deteriorate system performance, or even cause instability [33], [34]. Barrier Lyapunov function (BLF) originally proposed in [35] has been successfully utilized to handle such an issue in the context of multiagent networks [36]–[39]. Nevertheless, most existing literature in [36] and [39] require the agent dynamics to be in the form of low-order systems. The critical difficulty of extending the available BLF to high-order systems consists in how to construct some appropriate Lyapunov functions with well-imposed exponential powers. Despite two recent works in [40] and [41] were dedicated to solving this problem, they are neither suitable for multiagent networks nor do they consider the ETC. Motivated by the above discussions, the main innovative points of this work are listed as follows.

1) This seems to be a pioneering work of event-triggered-constrained consensus tracking design for high-order nonlinear multiagent networks in spite of ETC input and full-state constraints.
2) To overcome the difficulty that the existing event-triggered mechanisms in [23]–[32] cannot be used for high-order dynamics due to the presence of high-powers, a novel high-order event-triggered mechanism is for the first time formulated for (1) which is designed in combination with a new monotonically decreasing function that enables us to give a larger threshold to trigger the events as less as possible, while making the consensus tracking error smaller.
3) A high-order tan-type BLF is appropriately adopted to handle full-state constraints in the framework of the distributed adding-one-power-integrator control. Different from the existing results [18]–[22], we ensure that the full-state constraints are not transgressed while guaranteeing the boundedness of closed-loop networks.

II. Preliminaries and Problem Formulation

A. Algebraic Graph Theory

Let us first give some preliminaries on the graph theory. The communication topology among agents is described by a directed graph $\mathcal{G} = (\mathcal{V}, \mathcal{E})$ with $\mathcal{V} = \{v_0, v_1, \ldots, v_M\} (M \geq 2)$ and $\mathcal{E} \subseteq \mathcal{V} \times \mathcal{V}$ being the set of nodes (agents) and the set of edge, respectively. A directed edge $e_{ji} = (j, i) \in \mathcal{E}$ represents that agent i can obtain information from agent j. The neighbor set of agent i is denoted by $\mathcal{N}_i = \{j | e_{ji} \in \mathcal{E}\}$. Because agent 0 plays a special role (leader), let us consider the subgraph defined by $\overline{\mathcal{G}} = (\overline{\mathcal{V}}, \overline{\mathcal{E}})$ with $\overline{\mathcal{V}} = \{v_1, \ldots, v_M\}$ the set of follower agents and $\overline{\mathcal{E}} \subseteq \overline{\mathcal{V}} \times \overline{\mathcal{V}}$ defined accordingly. For this subgraph, let us define the adjacency matrix $\overline{\mathcal{A}} = [a_{ij}] \in \mathbb{R}^{M \times M}$ as follows: if $e_{ji} \in \overline{\mathcal{E}}$, then $a_{ij} > 0$; otherwise, $a_{ij} = 0$. The Laplacian matrix $\mathcal{L}$ associated with $\mathcal{G}$ is defined as $\mathcal{L} = \begin{bmatrix} 0 & \mathbf{0}_{M\times 1}^T \\ -\boldsymbol{\theta} & \overline{\mathcal{L}} + \mathcal{B} \end{bmatrix}$ with $\mathcal{B} = \text{diag}[\theta_1, \ldots, \theta_M]$, where $\theta_i > 0$ if the leader $0 \in \mathcal{N}_i, i = 1, \ldots, M$ and $\theta_i = 0$ otherwise. Moreover, $\boldsymbol{\theta} = [\theta_1, \ldots, \theta_M]^T$ and $\overline{\mathcal{L}} = \overline{\mathcal{D}} - \overline{\mathcal{A}}$ is the Laplacian matrix related to $\overline{\mathcal{L}}$ with $\overline{\mathcal{D}} = \text{diag}\{d_1, \ldots, d_M\} \in \mathbb{R}^{M \times M}$, where $d_i = \sum_{j \in \mathcal{N}_i} a_{ij}$. The directed graph $\mathcal{G}$ contains at least one directed spanning tree with the leader as the root [5]. It should be noted that $\overline{\mathcal{L}} + \mathcal{B}$ is a nonsingular $\mathcal{M}$-matrix [22].

B. Problem Statement

Consider a multiagent network whose follower agents have the following nonlinear dynamics:

$$\begin{cases} \dot{\chi}_{i,m} = \psi_{i,m}(\boldsymbol{\chi}_i) + \phi_{i,m}(\overline{\boldsymbol{\chi}}_{i,m})\chi_{i,m+1}^{p_{i,m}} \\ \dot{\chi}_{i,n_i} = \psi_{i,n_i}(\boldsymbol{\chi}_i) + \phi_{i,n_i}(\boldsymbol{\chi}_i)u_i^{p_{i,n_i}} \\ y_i = \chi_{i,1} \end{cases} \tag{1}$$

for $1 \leq i \leq M, 1 \leq m \leq n_i - 1$, where $\overline{\boldsymbol{\chi}}_{i,m} = [\chi_{i,1}, \chi_{i,2}, \ldots, \chi_{i,m}]^T \in \mathbb{R}^m$ and $\boldsymbol{\chi}_i = [\chi_{i,1}, \chi_{i,2}, \ldots, \chi_{i,n_i}]^T \in \mathbb{R}^{n_i}$ are the states, $y_i \in \mathbb{R}$ and $u_i \in \mathbb{R}$ are the output and the input signal of the ith follower agent, respectively. The functions $\psi_{i,m}(\cdot)$ and $\phi_{i,m}(\cdot)$ are unknown smooth nonlinearities, and $p_{i,m} \in Q_{\text{odd}}$, where Q_{odd} denotes the set of positive odd integers. All states remain within the following feasible set:

$$\Omega_{\chi_{i,m}} := \left\{\chi_{i,m} \in \mathbb{R}, \left|\chi_{i,m}(t)\right| \leq k_{b_{i,m}}\right\} \tag{2}$$

for some known upper bounds $k_{b_{i,m}} > 0$ $(1 \leq i \leq M,\ 1 \leq m \leq n_i)$.

Remark 1: The importance of the high-order nonlinear multiagent networks covers both theoretical and engineering aspects: from the theoretical point of view, the high-order nonlinear dynamics (1) generalize those of [3], [4], [8]–[10], [28], [30], [38], and [39] because the multiagent models in [3], [4], [8]–[10], [28], [30], [38], and [39] are a special case of (1) when $p_{i,m} = 1$. From the application point of view, dynamics (1) can describe relevant classes of practical systems, such as dynamical boiler-turbine units, hydraulic dynamics, poppet valve systems, or underactuated, weakly coupled mechanical systems with cubic force-deformation relations (nonlinear spring forces).

Control Objective: We aim to design an event-triggered consensus tracking control protocol for each follower agent such that each follower agent's output $y_i(t)$ can track the reference signal $y_L(t)$ with tunable tracking error. In addition, all signals of the closed-loop networks remain bounded as well as the full-state constraints are not violated.

At this point, the following assumptions and lemmas are first provided.

Assumption 1 [21]: For each follower agent i, we assume the sign of $\phi_{i,m}(\cdot)$ is positive and there exist known real constants $\underline{\phi}_{i,m} > 0$ and $\overline{\phi}_{i,m} > 0$, $(1 \le m \le n_i)$ satisfy $\underline{\phi}_{i,m} \le |\phi_{i,m}(\cdot)| \le \overline{\phi}_{i,m}$.

Assumption 2 [37]: For a continuously differentiable reference signal $y_L(t)$ of leader agent 0, there exist known positive constants $y_L^* < k_{b_{i,m}}$ and $y_{L,1}^*$ such that $|y_L| \le y_L^*$ and $|\dot{y}_L| \le y_{L,1}^*$.

Remark 2: Assumption 1 is given to ensure the controllability of system (1). Assumption 2 is standard and can be found in [33] and [37]–[40]. It should be noted that for the state-constrained multiagent networks, it is essential to select suitable bounded reference signal $y_L(t)$ to be tracked. Thus, Assumption 2 is reasonable, and we can always provide a robust estimate about the upper bound of $y_L(t)$.

Lemma 1 [22]: For any $\chi_1, \chi_2 \in \mathbb{R}$ and positive odd integer b, there exist real-valued functions $r_1(\cdot,\cdot)$ and $r_2(\cdot,\cdot)$ such that

$$(\chi_1 + \chi_2)^b = r_1(\chi_1, \chi_2)\chi_1^b + r_2(\chi_1, \chi_2)\chi_2^b$$

where $r_1(\chi_1, \chi_2) \in [\underline{\wp}_1, \overline{\wp}_1]$ with $\underline{\wp}_1 = 1 - \epsilon$ and $\overline{\wp}_1 = \max\{1 + \epsilon, 2^{b-1}\}$, with $\forall \epsilon \in (0, 1)$ a constant, $|r_2(\chi_1, \chi_2)| \le \wp_2$ with constant $\wp_2 > 0$ independent of χ_1 and χ_2.

Lemma 2 [26]: The hyperbolic tangent function $\tanh(\bullet)$ is continuous and differentiable, for any $\delta > 0$ and $\chi \in \mathbb{R}$, it has

$$0 \le |\chi| - \chi \tanh\left(\frac{\chi}{\delta}\right) \le \kappa\delta, \quad -\chi \tanh\left(\frac{\chi}{\delta}\right) \le 0$$

where $\kappa = \sup_{t>0}\{(t/[1 + e^t])\} = 0.2785$.

Lemma 3 [18]: Let $\zeta_1 \in \mathbb{R}$, $\zeta_2 \in \mathbb{R}$, and r_1 and r_2 be positive constants. For any $\varpi > 0$, it holds that

$$|\zeta_1|^{r_1}|\zeta_2|^{r_2} \le \frac{r_1\varpi|\zeta_1|^{r_1+r_2}}{r_1 + r_2} + \frac{r_2\varpi^{-r_1/r_2}|\zeta_2|^{r_1+r_2}}{r_1 + r_2}.$$

Lemma 4 [40]: For a given positive constant m, and every $\zeta_1 \in \mathbb{R}$ and $\zeta_2 \in \mathbb{R}$, there holds

$$\left|\zeta_1^m - \zeta_2^m\right| \le \Im_m\left(|\zeta_1 - \zeta_2|^{m-1} + |\zeta_2|^{m-1}\right)|\zeta_1 - \zeta_2|$$

where $\Im_m = m(1 + 2^{m-3})$ is a positive constant.

C. Fuzzy Logic Systems

Define a set of fuzzy IF-THEN rules, where the ith IF-THEN rule is written as [42] follows.

$\mathcal{R}^i$: If Z_1 is F_1^i and, ..., and Z_n is F_n^i, then y is B^i, where $\mathbf{Z} = [Z_1, \ldots, Z_n]^T \in \mathbb{R}^n$, and $y \in \mathbb{R}$ are the input and output of the FLSs, respectively, and $F_1^i, \ldots, F_n^i$ and B^i are fuzzy sets in $\mathbb{R}$. Let $h(\mathbf{Z})$ be a continuous function defined on a compact set $\Omega_{\mathbf{Z}}$. Then, for a given desired level of accuracy $\kappa > 0$, there exists an FLS $\boldsymbol{W}^{*T}\boldsymbol{S}(\mathbf{Z})$ such that $\sup_{\mathbf{Z}\in\Omega_{\mathbf{Z}}} |h(\mathbf{Z}) - \boldsymbol{W}^T\boldsymbol{S}(\mathbf{Z})| \le \kappa$, where $\boldsymbol{W} = [\varpi_1, \ldots, \varpi_f]^T$ is the adaptive fuzzy parameter vector in a compact set $\Omega_{\boldsymbol{W}}$. f is the number of the fuzzy rules. $\boldsymbol{S}(\mathbf{Z}) = [\psi_1(\mathbf{Z}), \ldots, \psi_f(\mathbf{Z})]^T$ is the fuzzy basis function vector with $\psi_i(\mathbf{Z}) = \Pi_{j=1}^n \mu_{F_j^i}(Z_j)/\sum_{i=1}^N [\Pi_{j=1}^n \mu_{F_j^i}(Z_j)]$, where $\mu_{F_j^i}(Z_j)$ is a fuzzy membership function of the variable Z_j in the IF-THEN rule. Let $\boldsymbol{W}^*$ be the optimal parameter vector, which is defined as

$$\boldsymbol{W}^* = \arg\min_{\boldsymbol{W}\in\Omega_W}\left\{\sup_{\mathbf{Z}\in\Omega_{\mathbf{Z}}}\left|h(\mathbf{Z}) - \boldsymbol{W}^T\boldsymbol{S}(\mathbf{Z})\right|\right\}.$$

Then, we can further obtain

$$h(\mathbf{Z}) = \boldsymbol{W}^{*T}\boldsymbol{S}(\mathbf{Z}) + \kappa \tag{3}$$

where κ is the minimum fuzzy approximation error.

III. Distributed Event-Triggered-Constrained Consensus Protocol Design

The distributed adding-one-power-integrator method, combined with high-order tan-type BLFs and a new high-order event-triggered mechanism, will be employed to facilitate the following control design. Define a constant $q_i = \max_{1\le m\le n_i}\{p_{i,m}\}(i = 1, 2, \ldots, M)$. Before moving on, the following transformation is given:

$$\begin{cases} s_{i,1} = \sum_{j\in\mathcal{N}_i} a_{ij}\big(y_i - y_j\big) + \theta_i(y_i - y_L) \\ s_{i,m} = \chi_{i,m} - \chi_{i,m,c}, \ \ m = 2, 3, \ldots, n_i \end{cases} \tag{4}$$

where $i = 1, \ldots, M$, and $x_{i,m,c}$ represents the virtual control inputs specified later. Moreover, $|\chi_{i,m,c}| < \chi_{i,m,c}^*$ is established, where $\chi_{i,m,c}^* > 0$ is a constant. After collecting $\boldsymbol{s}_1 = [s_{1,1}, s_{2,1}, \ldots, s_{M,1}]^T \in \mathbb{R}^M$, one has $\boldsymbol{s}_1 = (\overline{\mathcal{L}} + \mathcal{B})\boldsymbol{\delta}$ where $\boldsymbol{\delta} = \bar{\boldsymbol{y}} - \bar{\boldsymbol{y}}_L$ with $\bar{\boldsymbol{y}} = [y_1, y_2, \ldots, y_M]^T$ and $\bar{\boldsymbol{y}}_L = [y_L, y_L, \ldots, y_L]^T$. Because $\overline{\mathcal{L}} + \mathcal{B}$ is nonsingular, one has $\|\boldsymbol{\delta}\| \le (\|\boldsymbol{s}_1\|/[\underline{\sigma}(\overline{\mathcal{L}} + \mathcal{B})])$, being $\underline{\sigma}(\overline{\mathcal{L}} + \mathcal{B})$ the minimum singular value of $\overline{\mathcal{L}} + \mathcal{B}$.

A. Distributed-Constrained Consensus Protocol Design

Step i, 1 ($i \in \{1, \ldots, M\}$): The time derivative of $s_{i,1}$ along (1) and (4) is

$$\begin{aligned}\dot{s}_{i,1} = &-\sum_{j\in\mathcal{N}_i} a_{ij}\Big(\phi_{j,1}\big(\chi_{j,1}\big)\chi_{j,2}^{p_{j,1}} + \psi_{j,1}\big(\boldsymbol{\chi}_j\big)\Big) - \theta_i\dot{y}_L \\ &+ (d_i + \theta_i)\Big(\phi_{i,1}\big(\chi_{i,1}\big)\chi_{i,2}^{p_{i,1}} + \psi_{i,1}\big(\boldsymbol{\chi}_i\big)\Big).\end{aligned} \tag{5}$$

Take the high-order tan-type BLF as

$$V_{i,1} = \frac{2k_{c_{i,1}}^{q_i-p_{i,1}+2}}{\pi\big(q_i - p_{i,1} + 2\big)}\tan\left(\frac{\pi s_{i,1}^{q_i-p_{i,1}+2}}{2k_{c_{i,1}}^{q_i-p_{i,1}+2}}\right) + \frac{\widetilde{\beta}_{i,1}^2}{2\gamma_{i,1}} \tag{6}$$

where $k_{c_{i,1}} = (\sum_{j\in\mathcal{N}_i} a_{ij} + \theta_i)k_{b_{i,1}} - \sum_{j\in\mathcal{N}_i} a_{ij}y_{L,2}^* - \theta_i y_L^*$ is an upper bound of $s_{i,1}$ defined in a set $\Omega_{s_{i,1}} = \{s_{i,1}||s_{i,1}| < k_{c_{i,1}}\}$ with $y_{L,2}^*$ being a constant specified later. $\widetilde{\beta}_{i,1} = \beta_{i,1} - \hat{\beta}_{i,1}$ and $\gamma_{i,1} > 0$ is a design parameter.

Remark 3: If $k_{c_{i,m}} \to \infty$ approaches to infinity, the term $([2k_{c_{i,1}}^{q_i-p_{i,1}+2}]/[\pi(q_i - p_{i,1} + 2)])\tan(([\pi s_{i,1}^{q_i-p_{i,1}+2}]/[2k_{c_{i,1}}^{q_i-p_{i,1}+2}]))$ will tend to $([s_{i,1}^{q_i-p_{i,1}+2}]/[q_i - p_{i,1} + 2])$, thus the proposed controller can deal with both the constrained case and the unconstrained case. The conventional BLF-based controllers in [33]–[36] can only handle the constrained case due to the fact $\lim_{k_{c_{i,1}}\to\infty}(1/[q_i-p_{i,1}+2])\log([k_{c_{i,1}}^{q_i-p_{i,1}+2}]/[k_{c_{i,1}}^{q_i-p_{i,1}+2}-s_{i,1}^{q_i-p_{i,1}+2}])=0$.

Remark 4: In contrast with [40] and [41], the proposed high-order tan-type BLF method is more general in the sense that the existing BLF control protocol can be included as special cases of (6) when $p_{i,m}=1$, i.e., $k_{c_{i,1}}^2\tan[\pi s_{i,1}^2/2k_{c_{i,1}}^2]/\pi$. Thus, it can be also utilized to deal with the state-constrained control problem of low/high-order nonlinear multiagent networks.

In view of (5) and (6), the time derivative of $V_{i,1}$ is

$$\begin{aligned}\dot V_{i,1}=&-k_{i,1}\tan\left(\frac{\pi s_{i,1}^{q_i-p_{i,1}+2}}{2k_{c_{i,1}}^{q_i-p_{i,1}+2}}\right)-\frac{\widetilde\beta_{i,1}\dot{\widehat\beta}_{i,1}}{\gamma_{i,1}}-(d_i+\theta_i)l_{i,1}s_{i,1}^{q_i+1}\\&+\frac{s_{i,1}^{q_i-p_{i,1}+1}}{\Xi_{i,1}}\Big((d_i+\theta_i)\phi_{i,1}(\chi_{i,1})\chi_{i,2,c}^{p_{i,1}}+\mathcal F_{i,1}(\mathbf Z_{i,1})\Big)\\&+\frac{s_{i,1}^{q_i-p_{i,1}+1}}{\Xi_{i,1}}(d_i+\theta_i)\phi_{i,1}(\chi_{i,1})\Big(\chi_{i,2}^{p_{i,1}}-\chi_{i,2,c}^{p_{i,1}}\Big)\end{aligned}\tag{7}$$

where $\mathcal F_{i,1}(\mathbf Z_{i,1})=-\sum_{j\in\mathcal N_i}a_{ij}(\phi_{j,1}(\chi_{j,1})\chi_{j,2}^{p_{j,1}}+\psi_{j,1}(\boldsymbol\chi_j))-\theta_i\dot y_L+(d_i+\theta_i)(\psi_{i,1}(\boldsymbol\chi_i)+\Xi_{i,1}l_{i,1}s_{i,1}^{p_{i,1}})+k_{i,1}s_{i,1}^{-(q_i-p_{i,1}+1)}\sin([\pi s_{i,1}^{q_i-p_{i,1}+2}]/[2k_{c_{i,1}}^{q_i-p_{i,1}+2}])\cos([\pi s_{i,1}^{q_i-p_{i,1}+2}]/[2k_{c_{i,1}}^{q_i-p_{i,1}+2}])$, $\Xi_{i,1}=\cos^2([\pi s_{i,1}^{q_i-p_{i,1}+2}]/[2k_{c_{i,1}}^{q_i-p_{i,1}+2}])$ and $\mathbf Z_{i,1}=[\boldsymbol\chi_i^T,\boldsymbol\chi_j^T,y_L,\dot y_L]^T$.

An FLS $\boldsymbol W_{i,1}^{*T}\boldsymbol S_{i,1}(\mathbf Z_{i,1})$ is utilized to approximate $\mathcal F_{i,1}(\mathbf Z_{i,1})$, such that for any given $\kappa_{i,1}>0$, it holds that

$$\mathcal F_{i,1}(\mathbf Z_{i,1})=\boldsymbol W_{i,1}^{*T}\boldsymbol S_{i,1}(\mathbf Z_{i,1})+o_{i,1}(\mathbf Z_{i,1}),\ |o_{i,1}(\mathbf Z_{i,1})|\le\kappa_{i,1}\tag{8}$$

where $o_{i,1}(\mathbf Z_{i,1})$ is the approximation error.

Remark 5: As for $\mathcal F_{i,1}(\mathbf Z_{i,1})$, it has $\sin([\pi s_{i,1}^{q_i-p_{i,1}+2}]/[2k_{c_{i,1}}^{q_i-p_{i,1}+2}])\sim([\pi s_{i,1}^{q_i-p_{i,1}+2}]/[2k_{c_{i,1}}^{q_i-p_{i,1}+2}])$ when $s_{i,1}\to 0$. In the presence of this, one has

$$\begin{aligned}&\lim_{s_{i,1}\to 0}\frac{k_{i,1}}{s_{i,1}^{q_i-p_{i,1}+1}}\sin\left(\frac{\pi s_{i,1}^{q_i-p_{i,1}+2}}{2k_{c_{i,1}}^{q_i-p_{i,1}+2}}\right)\cos\left(\frac{\pi s_{i,1}^{q_i-p_{i,1}+2}}{2k_{c_{i,1}}^{q_i-p_{i,1}+2}}\right)\\&=\lim_{s_{i,1}\to 0}\frac{k_{i,1}\pi s_{i,1}}{2k_{c_{i,1}}^{q_i-p_{i,1}+2}}\cos\left(\frac{\pi s_{i,1}^{q_i-p_{i,1}+2}}{2k_{c_{i,1}}^{q_i-p_{i,1}+2}}\right)=0.\end{aligned}$$

It means that the singularity issue never emerges in $\mathcal F_{i,1}(\mathbf Z_{i,1})$. Thus, $\mathcal F_{i,1}(\mathbf Z_{i,1})$ is a continuous function and can be approximated by an FLS.

In light of Lemma 3, we get

$$\begin{aligned}\frac{s_{i,1}^{q_i-p_{i,1}+1}}{\Xi_{i,1}}\mathcal F_{i,1}=&\frac{s_{i,1}^{q_i-p_{i,1}+1}}{\Xi_{i,1}}\boldsymbol W_{i,1}^{*T}\boldsymbol S_{i,1}+\frac{s_{i,1}^{q_i-p_{i,1}+1}}{\Xi_{i,1}}o_{i,1}\\\le&\frac{1}{\bar p_{i,1}}\Gamma_{i,1}^{\bar p_{i,1}}\Xi_{i,1}^{-\bar p_{i,1}}\|\boldsymbol W_{i,1}^*\|^{\bar p_{i,1}}\|\boldsymbol S_{i,1}\|^{\bar p_{i,1}}s_{i,1}^{q_i+1}\\&+\frac{1}{\underline p_{i,1}}\Gamma_{i,1}^{-\underline p_{i,1}}\\&+\frac{1}{\underline p_{i,1}}\omega_{i,1}^{-\underline p_{i,1}}\kappa_{i,1}^{\underline p_{i,1}}+\frac{1}{\bar p_{i,1}}\omega_{i,1}^{\bar p_{i,1}}\Xi_{i,1}^{-\bar p_{i,1}}s_{i,1}^{q_i+1}\\\le&s_{i,1}^{q_i+1}\Xi_{i,1}^{-\bar p_{i,1}}\Big(\Gamma_{i,1}^{\bar p_{i,1}}\beta_{i,1}\Phi_{i,1}^{\bar p_{i,1}}+\omega_{i,1}^{\bar p_{i,1}}\Big)+\Theta_{i,1}\end{aligned}\tag{9}$$

where $\bar p_{i,1}=([q_i+1]/[q_i-p_{i,1}+1])$, $\underline p_{i,1}=([q_i+1]/p_{i,1})$, $\|\boldsymbol S_{i,1}\|=\Phi_{i,1}$, $\beta_{i,1}=\|\boldsymbol W_{i,1}^*\|^{\bar p_{i,1}}$, and $\Theta_{i,1}=\Gamma_{i,1}^{-\underline p_{i,1}}+\omega_{i,1}^{-\underline p_{i,1}}\kappa_{i,1}^{\underline p_{i,1}}$. It follows from (7)–(9) that the time derivative of $V_{i,1}$ is:

$$\begin{aligned}\dot V_{i,1}\le&-k_{i,1}\tan\left(\frac{\pi s_{i,1}^{q_i-p_{i,1}+2}}{2k_{c_{i,1}}^{q_i-p_{i,1}+2}}\right)-(d_i+\theta_i)l_{i,1}s_{i,1}^{q_i+1}\\&+\frac{s_{i,1}^{q_i-p_{i,1}+1}}{\Xi_{i,1}}(d_i+\theta_i)\phi_{i,1}(\chi_{i,1})\Big(\chi_{i,2}^{p_{i,1}}-\chi_{i,2,c}^{p_{i,1}}\Big)\\&-\frac{\widetilde\beta_{i,1}\dot{\widehat\beta}_{i,1}}{\gamma_{i,1}}+s_{i,1}^{q_i+1}\Xi_{i,1}^{-\bar p_{i,1}}\Big(\Gamma_{i,1}^{\bar p_{i,1}}\beta_{i,1}\Phi_{i,1}^{\bar p_{i,1}}+\omega_{i,1}^{\bar p_{i,1}}\Big)\\&+\frac{s_{i,1}^{q_i-p_{i,1}+1}}{\Xi_{i,1}}(d_i+\theta_i)\phi_{i,1}(\chi_{i,1})\chi_{i,2,c}^{p_{i,1}}+\Theta_{i,1}.\end{aligned}\tag{10}$$

Design the virtual control $\chi_{i,2,c}$ and the adaptive law $\dot{\widehat\beta}_{i,1}$ as

$$\begin{aligned}\chi_{i,2,c}&=-s_{i,1}\Big[\Re_{i,1}\Big(\Gamma_{i,1}^{\bar p_{i,1}}\widehat\beta_{i,1}\Phi_{i,1}^{\bar p_{i,1}}+\omega_{i,1}^{\bar p_{i,1}}\Big)\Big]^{\frac{1}{p_{i,1}}}\\&=-s_{i,1}\vartheta_{i,1}\end{aligned}\tag{11}$$

$$\Re_{i,1}=\Xi_{i,1}^{-\bar q_{i,1}}\Big[\underline\phi_{i,1}(d_i+\theta_i)\Big]^{-1}\tag{12}$$

$$\dot{\widehat\beta}_{i,1}=\Xi_{i,1}^{-\bar p_{i,1}}\gamma_{i,1}\Gamma_{i,1}^{\bar p_{i,1}}s_{i,1}^{q_i+1}\Phi_{i,1}^{\bar p_{i,1}}-\gamma_{i,1}\upsilon_{i,1}\widehat\beta_{i,1}\tag{13}$$

where $\bar q_{i,1}=(p_{i,1}/[q_i-p_{i,1}+1])$, $\Gamma_{i,1}$, $\upsilon_{i,1}$, $\omega_{i,1}$, and $\gamma_{i,1}$ are positive design constants. Substituting (11)–(13) into (10) yields

$$\begin{aligned}\dot V_{i,1}\le&-k_{i,1}\tan\left(\frac{\pi s_{i,1}^{q_i-p_{i,1}+2}}{2k_{c_{i,1}}^{q_i-p_{i,1}+2}}\right)-(d_i+\theta_i)l_{i,1}s_{i,1}^{q_i+1}\\&+\frac{s_{i,1}^{q_i-p_{i,1}+1}}{\Xi_{i,1}}(d_i+\theta_i)\phi_{i,1}(\chi_{i,1})\Big(\chi_{i,2}^{p_{i,1}}-\chi_{i,2,c}^{p_{i,1}}\Big)\\&+\upsilon_{i,1}\widetilde\beta_{i,1}\widehat\beta_{i,1}+\Theta_{i,1}.\end{aligned}\tag{14}$$

According to Lemmas 3 and 4, we have

$$\begin{aligned}&\frac{s_{i,1}^{q_i-p_{i,1}+1}}{\Xi_{i,1}}\phi_{i,1}(\chi_{i,1})\Big(\chi_{i,2}^{p_{i,1}}-\chi_{i,2,c}^{p_{i,1}}\Big)\\&\le\frac{s_{i,1}^{q_i-p_{i,1}+1}}{\Xi_{i,1}}\overline\phi_{i,1}\Im_{p_{i,1}}\Big(|s_{i,2}|^{p_{i,1}}+(s_{i,1}\vartheta_{i,1})^{p_{i,1}-1}|s_{i,2}|\Big)\\&\le\frac{1}{\underline p_{i,1}}\zeta_{i,1}\overline\phi_{i,1}^{\underline p_{i,1}}\Xi_{i,1}^{-\underline p_{i,1}}s_{i,2}^{q_i+1}+\frac{1}{\bar p_{i,1}}\zeta_{i,1}^{-\bar q_{i,1}}\Im_{p_{i,1}}^{\bar p_{i,1}}s_{i,1}^{q_i+1}\\&+\frac{1}{q_i+1}\zeta_{i,1}\Xi_{i,1}^{-(q_i+1)}s_{i,2}^{q_i+1}\Big(\overline\phi_{i,1}\vartheta_{i,1}^{p_{i,1}-1}\Big)^{q_i+1}\\&+\frac{q_i}{q_i+1}\zeta_{i,1}^{-\frac{1}{q_i}}\Im_{p_{i,1}}^{\frac{q_i+1}{q_i}}s_{i,1}^{q_i+1}\\&\le l_{i,1}s_{i,1}^{q_i+1}+(d_i+\theta_i)^{-1}\overline\vartheta_{i,1}s_{i,2}^{q_i+1}\end{aligned}\tag{15}$$

where $l_{i,1}=(1/\bar p_{i,1})\zeta_{i,1}^{-\bar q_{i,1}}\Im_{p_{i,1}}^{\bar p_{i,1}}+(q_i/[q_i+1])\ \zeta_{i,1}^{-(1/q_i)}\Im_{p_{i,1}}^{([q_i+1]/q_i)}$ and $\overline\vartheta_{i,1}=(1/\underline p_{i,1})\ (d_i+\theta_i)\ \zeta_{i,1}(\overline\phi_{i,1}/\Xi_{i,1})^{\underline p_{i,1}}+$

$(d_i+\theta_i)$ $(1/[q_i+1])$ $\zeta_{i,1}(([\overline{\phi}_{i,1}\vartheta_{i,1}^{p_{i,1}-1}]/\Xi_{i,1}))^{q_i+1}$ with $\Im_{p_{i,1}} = p_{i,1}(1+2^{p_{i,1}-3})$ and $\zeta_{i,1}$ is a constant. Applying Young's inequality to $\upsilon_{i,1}\widetilde{\beta}_{i,1}\widehat{\beta}_{i,1}$ and considering (15), one arrives at

$$\dot{V}_{i,1} \le -k_{i,1}\tan\left(\frac{\pi s_{i,1}^{q_i-p_{i,1}+2}}{2k_{c_{i,1}}^{q_i-p_{i,1}+2}}\right) + s_{i,2}^{q_i+1}\overline{\vartheta}_{i,1} + \frac{1}{2}\upsilon_{i,1}\left(\beta_{i,1}^2-\widetilde{\beta}_{i,1}^2\right) + \Theta_{i,1}. \quad (16)$$

Step i, m ($i \in \{1,\ldots,M\}, m \in \{2,\ldots,n_i-1\}$): By means of (1) and (4), we obtain the time derivative of $s_{i,m}$ as

$$\dot{s}_{i,m} = \phi_{i,m}(\overline{\boldsymbol{\chi}}_{i,m})\chi_{i,m+1}^{p_{i,m}} + \psi_{i,m}(\boldsymbol{\chi}_i) - \dot{\chi}_{i,m,c}. \quad (17)$$

The following finite-time-convergent differentiator (FTCD) is then utilized to estimate $\dot{\chi}_{i,m,c}$:

$$\begin{cases}\dot{\chi}_{i,m,c}^c = \dot{\chi}_{i,m,c}^d - \ell_{i,m-1}^a \varkappa_{i,m-1}^a \\ \dot{\chi}_{i,m,c}^d = -\ell_{i,m-1}^b \varkappa_{i,m-1}^b\end{cases} \quad (18)$$

with $\chi_{i,m,c}^c$ and $\dot{\chi}_{i,m,c}^c$ being the estimates of $\chi_{i,m,c}$ and $\dot{\chi}_{i,m,c}$, respectively, and

$$\begin{cases}\varkappa_{i,m-1}^a = |z_{i,m-1}|^{\frac{1}{2}}\operatorname{sign}(z_{i,m-1}) + \hbar_{i,m-1}z_{i,m-1} \\ \varkappa_{i,m-1}^b = -\hbar_{i,m-1}|z_{i,m-1}|^{\frac{1}{2}}\operatorname{sign}(z_{i,m-1}) \\ \qquad + \hbar_{i,m-1}^2 z_{i,m-1} + \operatorname{sign}(z_{i,m-1})\end{cases} \quad (19)$$

where $z_{i,m-1} = \chi_{i,m,c} - \chi_{i,m,c}^c$ denotes the estimation error, and $\ell_{i,m-1}^a$, $\ell_{i,m-1}^b$, $\hbar_{i,m-1}$ are positive design constants, and sign($\bullet$) is the signum function. According to the discussion in [43], for any given $\varsigma_{i,m-1}^* > 0$, the following equation holds:

$$\dot{\chi}_{i,m,c} = \dot{\chi}_{i,m,c}^c + \varsigma_{i,m-1}, \quad |\varsigma_{i,m-1}| \le \varsigma_{i,m-1}^* \quad (20)$$

where $\varsigma_{i,m-1}$ is the estimation error of the FTCD. Take the high-order tan-type BLFs as

$$V_{i,m} = V_{i,m-1} + \frac{2k_{c_{i,m}}^{q_i-p_{i,m}+2}}{\pi(q_i-p_{i,m}+2)}\tan\left(\frac{\pi s_{i,m}^{q_i-p_{i,m}+2}}{2k_{c_{i,m}}^{q_i-p_{i,m}+2}}\right) + \frac{1}{2\gamma_{i,m}}\widetilde{\beta}_{i,m}^2 \quad (21)$$

where $k_{c_{i,m}} = k_{b_{i,m}} - \chi_{i,m,c}^*$ is an upper bound of $s_{i,m}$ defined in a set $\Omega_{s_{i,m}} = \{s_{i,m}||s_{i,m}| < k_{c_{i,m}}\}$ with $\chi_{i,m,c}^*$ being a constant specified later. $\widetilde{\beta}_{i,m} = \beta_{i,m} - \widehat{\beta}_{i,m}$ and $\gamma_{i,m} > 0$ is a design parameter. It follows from (17), (20), and (21) that the time derivative of $V_{i,m}$ is:

$$\begin{aligned}\dot{V}_{i,m} \le{}& \frac{s_{i,m}^{q_i-p_{i,m}+1}}{\Xi_{i,m}}\left(\phi_{i,m}(\overline{\boldsymbol{\chi}}_{i,m})\chi_{i,m+1,c}^{p_{i,m}} - \varsigma_{i,m-1}^* + \mathcal{F}_{i,m}(\mathbf{Z}_{i,m})\right) \\ &+ \sum_{n=1}^{m-1}\Theta_{i,n} + \frac{s_{i,m}^{q_i-p_{i,m}+1}}{\Xi_{i,m}}\phi_{i,m}(\overline{\boldsymbol{\chi}}_{i,m})\left(\chi_{i,m+1}^{p_{i,m}} - \chi_{i,m+1,c}^{p_{i,m}}\right) \\ &+ \sum_{n=1}^{m-1}\left(\frac{1}{2}\upsilon_{i,n}\left(\beta_{i,n}^2 - \widetilde{\beta}_{i,n}^2\right)\right) - \frac{s_{i,m}^{q_i-p_{i,m}+1}}{\Xi_{i,m}}\dot{\chi}_{i,m,c}^c \\ &- \sum_{n=1}^{m} k_{i,n}\tan\left(\frac{\pi s_{i,n}^{q_i-p_{i,n}+2}}{2k_{c_{i,n}}^{q_i-p_{i,n}+2}}\right) - \frac{\widetilde{\beta}_{i,m}\dot{\widehat{\beta}}_{i,m}}{\gamma_{i,m}} \\ &- l_{i,m}s_{i,m}^{q_i+1} + \overline{\vartheta}_{i,m-1}s_{i,m}^{q_i+1} \end{aligned} \quad (22)$$

where $\mathcal{F}_{i,m}(\mathbf{Z}_{i,m}) = \sin([\pi s_{i,m}^{q_i-p_{i,m}+2}]/[2k_{c_{i,m}}^{q_i-p_{i,m}+2}])$ $\cos([\pi s_{i,m}^{q_i-p_{i,m}+2}]/[2k_{c_{i,m}}^{q_i-p_{i,m}+2}])$ $k_{i,m}s_{i,m}^{-(q_i-p_{i,m}+1)} + \psi_{i,m}(\boldsymbol{\chi}_i) + \Xi_{i,m}l_{i,m}s_{i,m}^{p_{i,m}}$, $\Xi_{i,m} = \cos^2([\pi s_{i,m}^{q_i-p_{i,m}+2}]/[2k_{c_{i,m}}^{q_i-p_{i,m}+2}])$, and $\mathbf{Z}_{i,m} = [\boldsymbol{\chi}_i^T, \boldsymbol{\chi}_j^T, \widehat{\beta}_{i,1}, \widehat{\beta}_{i,2}, \ldots, \widehat{\beta}_{i,m-1}, y_L, \dot{y}_L, \ddot{y}_L]^T$. Analogous to step 1, one has

$$\begin{aligned}\frac{s_{i,m}^{q_i-p_{i,m}+1}}{\Xi_{i,m}}\mathcal{F}_{i,m} ={}& \frac{s_{i,m}^{q_i-p_{i,m}+1}}{\Xi_{i,m}}\left(\boldsymbol{W}_{i,m}^{*T}\boldsymbol{S}_{i,m} + o_{i,m}\right) \\ \le{}& s_{i,m}^{q_i+1}\Xi_{i,m}^{-\bar{p}_{i,m}}\Gamma_{i,m}^{\bar{p}_{i,m}}\beta_{i,m}\Phi_{i,m}^{\bar{p}_{i,m}} + \omega_{i,m}^{-\underline{p}_{i,m}}\kappa_{i,m}^{\underline{p}_{i,m}} \\ &+ s_{i,m}^{q_i+1}\Xi_{i,m}^{-\bar{p}_{i,m}}\omega_{i,m}^{\bar{p}_{i,m}} + \delta_{i,m}^{-\underline{p}_{i,m}} \end{aligned} \quad (23)$$

where $\|\boldsymbol{S}_{i,m}\| = \Phi_{i,m}$ and $\beta_{i,m} = \|\boldsymbol{W}_{i,m}^*\|^{\bar{p}_{i,m}}$. Besides, applying Lemma 3 yields $-s_{i,m}^{q_i-p_{i,m}+1}\Xi_{i,m}^{-1}\varsigma_{i,m-1} \le s_{i,m}^{q_i+1}\Xi_{i,m}^{-\bar{p}_{i,m}}\xi_{i,m}^{\bar{p}_{i,m}} + \xi_{i,m}^{-\underline{p}_{i,m}}\varsigma_{i,m-1}^{*\underline{p}_{i,m}}$. For subsequent analysis, let us define $\Theta_{i,m} = \Gamma_{i,m}^{-\underline{p}_{i,m}} + \omega_{i,m}^{-\underline{p}_{i,m}}\kappa_{i,m}^{\underline{p}_{i,m}} + \xi_{i,m}^{-\underline{p}_{i,m}}\varsigma_{i,m-1}^{*\underline{p}_{i,m}}$ and $\bar{p}_{i,m} = ([q_i+1]/[q_i-p_{i,m}+1])$, $\underline{p}_{i,m} = ([q_i+1]/p_{i,m})$. Design the virtual control input $\chi_{i,m+1,c}$ and the adaptive law $\dot{\widehat{\beta}}_{i,m}$ as

$$\begin{aligned}\chi_{i,m+1,c} ={}& -s_{i,m}\Big[\Re_{i,m}\Big(\Xi_{i,m}^{\bar{p}_{i,m}}\overline{\vartheta}_{i,m-1} + \Gamma_{i,m}^{\bar{p}_{i,m}}\widehat{\beta}_{i,m}\Phi_{i,m}^{\bar{p}_{i,m}} \\ &- s_{i,m}^{-p_{i,m}}\Xi_{i,m}^{\bar{q}_{i,m}}\dot{\chi}_{i,m,c}^c + \omega_{i,m}^{\bar{p}_{i,m}} + \xi_{i,m}^{\bar{p}_{i,m}}\Big)\Big]^{\frac{1}{p_{i,m}}} \\ ={}& -s_{i,m}\vartheta_{i,m} \end{aligned} \quad (24)$$

$$\Re_{i,m} = \Xi_{i,m}^{-\bar{q}_{i,m}}\underline{\phi}_{i,m}^{-1} \quad (25)$$

$$\dot{\widehat{\beta}}_{i,m} = \Xi_{i,m}^{-\bar{p}_{i,m}}\gamma_{i,m}\Gamma_{i,m}^{\bar{p}_{i,m}}s_{i,m}^{q_i+1}\Phi_{i,m}^{\bar{p}_{i,m}} - \gamma_{i,m}\upsilon_{i,m}\widehat{\beta}_{i,m} \quad (26)$$

where $\bar{q}_{i,m} = (p_{i,m}/[q_i-p_{i,m}+1])$, $\Gamma_{i,m}$, $\upsilon_{i,m}$, $\omega_{i,m}$, $\xi_{i,m}$, and $\gamma_{i,m}$ are positive design constants. Hence, the derivative of $V_{i,m}$ along (22)–(26) satisfies

$$\begin{aligned}\dot{V}_{i,m} \le{}& \sum_{n=1}^{m}\Theta_{i,n} - \sum_{n=1}^{m}k_{i,n}\tan\left(\frac{\pi s_{i,n}^{q_i-p_{i,n}+2}}{2k_{c_{i,n}}^{q_i-p_{i,n}+2}}\right) - l_{i,m}s_{i,m}^{q_i+1} \\ &+ \sum_{n=1}^{m-1}\left(\frac{1}{2}\upsilon_{i,n}\left(\beta_{i,n}^2 - \widetilde{\beta}_{i,n}^2\right)\right) + \upsilon_{i,m}\widetilde{\beta}_{i,m}\widehat{\beta}_{i,m} \\ &+ \frac{s_{i,m}^{q_i-p_{i,m}+1}}{\Xi_{i,m}}\phi_{i,m}(\overline{\boldsymbol{\chi}}_{i,m})\left(\chi_{i,m+1}^{p_{i,m}} - \chi_{i,m+1,c}^{p_{i,m}}\right). \end{aligned} \quad (27)$$

Using Lemmas 3 and 4, one reaches

$$\frac{s_{i,m}^{q_i-p_{i,m}+1}}{\Xi_{i,m}}\phi_{i,m}(\overline{\boldsymbol{\chi}}_{i,m})\left(\chi_{i,m+1}^{p_{i,m}} - \chi_{i,m+1,c}^{p_{i,m}}\right) \le l_{i,m}s_{i,m}^{q_i+1} + \overline{\vartheta}_{i,m}s_{i,m+1}^{q_i+1} \quad (28)$$

where $l_{i,m} = (1/\bar{p}_{i,m})\zeta_{i,m}^{-\bar{q}_{i,m}}\Im_{p_{i,m}}^{\bar{p}_{i,m}} + (q_i/[q_i+1])\zeta_{i,m}^{-(1/q_i)}$ $\Im_{p_{i,m}}^{([q_i+1]/q_i)}$, $\overline{\vartheta}_{i,m} = (1/\underline{p}_{i,m})\zeta_{i,m}(\overline{\phi}_{i,m}/\Xi_{i,m})^{\underline{p}_{i,m}} + (1/[q_i+1])$ $\zeta_{i,m}([\overline{\phi}_{i,m}\vartheta_{i,m}^{p_{i,m}-1}]/\Xi_{i,m})^{q_i+1}$ with $\Im_{p_{i,m}} = p_{i,m}(1+2^{p_{i,m}-3})$

and $\zeta_{i,m}$ is a constant. By employing Young's inequality to $\upsilon_{i,m}\widetilde{\beta}_{i,m}\widehat{\beta}_{i,m}$, and substituting (28) into (27) results in

$$\dot{V}_{i,m} \leq -\sum_{n=1}^{m} k_{i,n}\tan\left(\frac{\pi s_{i,n}^{q_i-p_{i,n}+2}}{2k_{c_{i,n}}^{q_i-p_{i,n}+2}}\right) + s_{i,m+1}^{q_i+1}\overline{\vartheta}_{i,m} + \sum_{n=1}^{m}\left(\frac{1}{2}\upsilon_{i,n}\left(\beta_{i,n}^2 - \widetilde{\beta}_{i,n}^2\right)\right) + \sum_{n=1}^{m}\Theta_{i,n}. \quad (29)$$

B. High-Order Event-Triggered Mechanism

In this section, we propose a new high-order event-triggered mechanism, and the ETC signal is given by

$$u_i(t) = \upsilon_i(t_h)\ \forall t \in \left[t_h, t_{h+1}\right) \quad (30)$$

where $\upsilon_i(t)$ is transition control signal. The high-order event-triggered mechanism is described as

$$t_{h+1} = \inf\left\{t > t_h \middle| |e_i(t)| \geq \delta_{i,0}\left|u_i^{\bar{q}_{i,n_i}}(t)\right| + \tau_{i,0} + \frac{\lambda_{i,0}}{\sum_{k=1}^{n}\left|s_{i,k}(t)\right| + \kappa_{i,0}}\right\} \quad (31)$$

where $e_i(t) = \upsilon_i(t) - u_i^{\bar{q}_{i,n_i}}(t)$ stands for the control sampling error with $\bar{q}_{i,n_i} = (p_{i,n_i}/[q_i - p_{i,n_i} + 1])$. $0 < \delta_{i,0} < 1$, $\lambda_{i,0}$, $\tau_{i,0}$, and $\kappa_{i,0}$ are positive design constants.

Define $s_{i,0}(t) = (1/[\sum_{k=1}^{n}|s_{i,k}(t)| + \kappa_{i,0}])$ and it can be known that $s_{i,0}$ is a monotonically decreasing function of the local tracking errors $s_{i,k}(t), k = 1, 2, \ldots, n_i$. From (30) and (31), it can be verified that $|\upsilon_i(t) - u_i^{\bar{q}_{i,n_i}}(t)| \leq \delta_{i,0}|u_i^{\bar{q}_{i,n_i}}(t)| + \tau_{i,0} + \lambda_{i,0}s_{i,0}(t)$ holds for all $t \in [t_h, t_{h+1})$. Then, the following two situations should be considered.

Situation I: When $u_i(t) \geq 0$. Since $u_i(t) > 0$, one can obtain

$$-\delta_{i,0}u_i^{\bar{q}_{i,n_i}}(t) - \lambda_{i,0}s_{i,0}(t) - \tau_{i,0} \leq \upsilon_i(t) - u_i^{\bar{q}_{i,n_i}}(t) \leq \delta_{i,0}u_i^{\bar{q}_{i,n_i}}(t) + \lambda_{i,0}s_{i,0}(t) + \tau_{i,0}. \quad (32)$$

Thus, it is possible to get that

$$\upsilon_i(t) - u_i^{\bar{q}_{i,n_i}}(t) = c_{i,0}(t)\left(\delta_{i,0}u_i^{\bar{q}_{i,n_i}}(t) + \tau_{i,0} + \lambda_{i,0}s_{i,0}(t)\right) \quad (33)$$

where $c_{i,0}(t)$ is a time-varying parameter satisfying $c_{i,0}(t) \in [-1, 1]$.

Situation II: When $u_i(t) < 0$, it is possible to reach

$$\delta_{i,0}u_i^{\bar{q}_{i,n_i}}(t) - \lambda_{i,0}s_{i,0}(t) - \tau_{i,0} \leq \upsilon_i(t) - u_i^{\bar{q}_{i,n_i}}(t) \leq -\delta_{i,0}u_i^{\bar{q}_{i,n_i}}(t) + \lambda_{i,0}s_{i,0}(t) + \tau_{i,0}. \quad (34)$$

Furthermore, we have

$$\upsilon_i(t) - u_i^{\bar{q}_{i,n_i}}(t) = c_{i,0}(t)\left(\delta_{i,0}u_i^{\bar{q}_{i,n_i}}(t) - \tau_{i,0} - \lambda_{i,0}s_{i,0}(t)\right). \quad (35)$$

Synthesizing and summarizing the above two situations lead to

$$\upsilon_i(t) - u_i^{\bar{q}_{i,n_i}}(t) \leq c_{i,2}(t)\left(\lambda_{i,0}s_{i,0}(t) + \tau_{i,0}\right) + c_{i,1}(t)\delta_{i,0}u_i^{\bar{q}_{i,n_i}}(t) \quad (36)$$

where

$$\begin{cases} c_{i,1}(t) = c_{i,2}(t) = c_{i,0}(t), u_i(t) \geq 0 \\ c_{i,1}(t) = c_{i,0}(t), c_{i,2}(t) = -c_{i,0}(t),\ u_i(t) < 0. \end{cases}$$

It is not hard to deduce that

$$u_i(t) = \left[\frac{\upsilon_i(t) - c_{i,2}(t)\lambda_{i,0}s_{i,0} - c_{i,2}(t)\tau_{i,0}}{1 + c_{i,1}(t)\delta_{i,0}}\right]^{\frac{1}{\bar{q}_{i,n_i}}}. \quad (37)$$

The transition control signal $\upsilon_i(t)$ is

$$\upsilon_i(t) = \left(1 + \delta_{i,0}\right)\left[\alpha_{i,n_i} - s_{i,0}\tanh\left(\frac{s_{i,0}s_{i,n_i}\Xi_{i,n_i}^{-\underline{q}_{i,n_i}}}{\delta_{i,1}}\right) - \delta_{i,2}\tanh\left(\frac{\delta_{i,2}s_{i,n_i}\Xi_{i,n_i}^{-\underline{q}_{i,n_i}}}{\delta_{i,1}}\right)\right] \quad (38)$$

$$\alpha_{i,n_i} = -s_{i,n_i}^{\bar{q}_{i,n_i}}\left[\Re_{i,n_i}\left(\Xi_{i,n_i}^{\bar{p}_{i,n_i}}\overline{\vartheta}_{i,n_i-1} + \Gamma_{i,n_i}^{\bar{p}_{i,n_i}}\widehat{\beta}_{i,n_i}\Phi_{i,n_i}^{\bar{p}_{i,n_i}} - s_{i,n_i}^{-p_{i,n_i}}\Xi_{i,n_i}^{\bar{q}_{i,n_i}}\dot{\chi}_{i,n_i,c}^{c} + \omega_{i,n_i}^{\bar{p}_{i,n_i}} + \xi_{i,n_i}^{\bar{p}_{i,n_i}}\right)\right]^{\underline{q}_{i,n_i}} \quad (39)$$

$$\Re_{i,n_i} = \Xi_{i,n_i}^{-\bar{q}_{i,n_i}}\left[\underline{\phi}_{i,n_i}(1-\epsilon)\right]^{-1} \quad (40)$$

where $\Xi_{i,n_i} = \cos^2([\pi s_{i,n_i}^{q_i-p_{i,n_i}+2}]/[2k_{c_{i,n_i}}^{q_i-p_{i,n_i}+2}])$, ω_{i,n_i}, Γ_{i,n_i}, ξ_{i,n_i} $\delta_{i,1}$, and $\delta_{i,2} > \delta_{i,0}$ are positive design constants satisfying $\lambda_{i,0} < 1 - \delta_{i,0}$, $\tau_{i,0} < \delta_{i,2}(1 - \delta_{i,0})$. Design the adaptive law $\widehat{\beta}_{i,n_i}$ as

$$\dot{\widehat{\beta}}_{i,n_i} = \Xi_{i,n_i}^{-\bar{p}_{i,n_i}}\gamma_{i,n_i}\Gamma_{i,n_i}^{\bar{p}_{i,n_i}}s_{i,n_i}^{q_i+1}\Phi_{i,n_i}^{\bar{p}_{i,n_i}} - \gamma_{i,n_i}\upsilon_{i,n_i}\widehat{\beta}_{i,n_i} \quad (41)$$

where $\bar{p}_{i,n_i} = ([q_i + 1]/[q_i - p_{i,n_i} + 1])$, $\underline{q}_{i,n_i} = (1/[q_i - p_{i,n_i} + 1])$, γ_{i,n_i} and υ_{i,n_i} are positive design constants.

Remark 6: To highlight the distinguishing feature of the newly proposed high-order event-triggering mechanism (31), we first briefly recall the existing designs in [23]–[32]. Note that state-of-the-art ETC signals are typically devised as $u_i(t) = ([\upsilon_i(t)]/[1 + c_{i,1}(t)\delta_{i,0}]) - ([c_{i,2}(t)\tau_{i,0}]/[1 + c_{i,1}(t)\delta_{i,0}])$ on the basis of Lemma 2. Such an idea relies on the precondition $s_{i,n_i}\upsilon_i(t) \leq 0$ so as to obtain $-\chi\tanh(\chi/\delta) \leq 0$. However, such a precondition cannot be satisfied for high-order case due to the existence of high powers $q_i - p_{i,n_i} + 1$ and p_{i,n_i} such as $s_{i,n_i}^{q_i-p_{i,n_i}+1}$ and $(([\upsilon_i(t)]/[1 + c_{i,1}(t)\delta_{i,0}]) - ([c_{i,2}(t)\tau_{i,0}]/[1 + c_{i,1}(t)\delta_{i,0}]))^{p_{i,n_i}}$. To solve this issue, we develop a high-order event-triggered mechanism as in (31) whose importance is listed in Remarks 7 and 8.

Remark 7: In contrast to conventional event-triggered strategies (e.g., fixed threshold, relative threshold, and switching threshold) [23]–[28], [30]–[32], our proposed triggering threshold exhibits a better balance between tracking accuracy and resource utilization. This is because existing thresholds in [23]–[28] and [30]–[32] are composed by the amplitudes of control signals as well as a fixed threshold. Such designs theoretically imply that tracking accuracy is weakened when the magnitudes of control signals become large. When the magnitudes of control signals are approaching zero, more precise control can be applied to the system such that better tracking accuracy can be obtained, however, which will make the threshold small. To tackle such contradiction, a monotonically decreasing function $s_{i,0}(t)$ in our article is embedded into the design of the proposed high-order event-triggered mechanism and its role is allowing a relatively big threshold, while guaranteeing that the consensus tracking error is small, and that singularity issue is precluded due to the use of $\kappa_{i,0}$ in (31).

Remark 8: When taking $p_{i,m} = 1$, dynamics (1) are the low-order nonlinear multiagent networks, and the high-order event-triggered strategy reduces to $t_{h+1} = \inf\{t > t_h || e_i(t)| \geq \delta_{i,0}|u_i(t)| + \tau_{i,0} + \lambda_{i,0}s_{i,0}(t)\}$ with $e_i(t) = \upsilon_i(t) - u_i(t)$, which is exactly the one suitable for low-order systems. Besides, (31) encompasses the existing event-triggered mechanism [24] (e.g., the fixed threshold strategy (12) and (13) or relative threshold (23) and (24) in [24]) as special cases when $\delta_{i,0} = \lambda_{i,0} = 0$ or $\lambda_{i,0} = 0$.

IV. Stability Analysis

At this point, the main result of this article is given in the following Theorem 1.

Theorem 1: For the high-order nonlinear multiagent networks (1) with full-state constraints, under Assumptions 1 and 2, consider the distributed event-triggered-constrained consensus tracking controllers (11), (12), (24), (25), and (38)–(40) and adaption laws (13), (26) and (41) with initial conditions $\chi_{i,m}(0) \in \Omega_{\chi_{i,m,0}} = \{\chi_{i,m}||\chi_{i,m}(0)| \leq k_{b_{i,m}}\}$ and $\widehat{\beta}_{i,m}(0) \geq 0, i = 1, 2, \ldots, M, m = 1, 2, \ldots, n_i$, it holds the following.

1) All closed-loop signals remain bounded, and system states $\chi_{i,m}$ can be confined within the compact set $\Omega_{\chi_{i,m}} := \{\chi_{i,m}||\chi_{i,m}(t)| \leq k_{b_{i,m}}\}$ all the time.
2) The consensus tracking error $\boldsymbol{\delta}$ eventually converges into the compact set Ω_s defined by

$$\Omega_s = \left\{ \|\boldsymbol{\delta}\| \leq \sqrt{\frac{1}{\underline{\sigma}^2(\mathcal{L}+\mathcal{B})}\sum_{i=1}^{M}\Lambda^2} \right\}$$

where Λ is a positive constant given later.
3) Zeno-behavior phenomenon is excluded in the sense that the interexecution intervals $\{t_{h+1} - t_h\}$ are lower bounded by a positive constant T_i^* $\forall h \in N^+$.

Proof: See the Appendix. ■

Remark 9: The size of Ω_s can be made small by decreasing $\Gamma_{i,m}$, $\omega_{i,m}$, $\xi_{i,m}$, and $\upsilon_{i,m}$, while increasing $\gamma_{i,m}$. Then, the design parameters $\Gamma_{i,m}$, $\omega_{i,m}$, $\upsilon_{i,m}$, $\xi_{i,m}$, and $\gamma_{i,m}$ can be adjusted so as to satisfy $(\varrho/\alpha) \leq \Pi$, namely, $V(t) \leq \Pi$ holds for $\forall t \geq 0$. Furthermore, a design procedure of the proposed algorithm can be sketched as follows.

Algorithm 1 Design Procedure of the Proposed Algorithm

1: Specify a constant $\Pi > 0$ and choose appropriate initial conditions $\chi_{i,m}(0)$ and $\widehat{\beta}_{i,m}(0) \geq 0$ for $i = 1, \ldots, M, m = 1, \ldots, n_i$ to satisfy $V(0) < \Pi$;
2: Define fuzzy rules, fuzzy sets, fuzzy membership functions, and then determine FLSs. Accordingly, calculate $\Phi_{i,m}$;
3: Assign specific values to the design parameters $\gamma_{i,m} > 0$, $\Gamma_{i,m} > 0$, $\omega_{i,m} > 0$, $\upsilon_{i,m} > 0$ and $\xi_{i,m} > 0$;
4: Determine the intermediate variables according to the following order: $s_{i,1} \to \widehat{\beta}_{i,1} \to \alpha_{i,2,c} \to s_{i,2} \to \widehat{\beta}_{i,2} \to \alpha_{i,3,c} \to s_{i,m} \to \widehat{\beta}_{i,m} \to \alpha_{i,m+1,c} \to \cdots \to s_{i,n_i} \to \widehat{\beta}_{i,n_i} \to u_i$ for $i = 1, 2, \ldots, M, m = 3, \ldots, n_i - 1$.

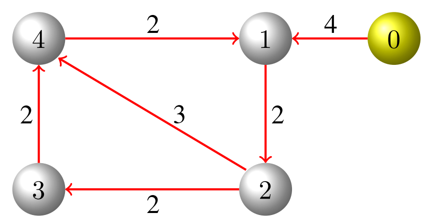

Fig. 1. Communication topology.

V. Simulation Example

To verify the effectiveness of the proposed scheme in practical application, a practical example composed of four different poppet valve systems [44] and a reference signal over the communication graph is considered, as shown in Fig. 1. From Fig. 1, it can be seen that the reference signal is accessible to the follower 1 only and is given by $y_L(t) = 5\sin(t) + 10\sin(0.5t)$.

The poppet valve system is one of the most commonly used components in hydraulic systems, which can be modeled by the annular leakage equation. The input force f_i drives the poppet to move along the y-axis, regulating the volumetric flow rate $h_i = \lambda_i \varpi_i^3$ of oil from high to low pressure chamber with $\lambda_i = (\pi l_i^*/6b_iD_i)\Delta P_i$ being a lumped coefficient and ϖ_i being the effective clearance of the annular passage. l_i^*, b_i, and D_i are constants independent of axial motion of the poppet. ΔP_i is the pressure drop between two chambers and remains almost unchanged in the control process.

According to the geometric structure, $\varpi_i = \epsilon_i x_i$ with ϵ_i being a constant related to the cone angle of poppet. The dynamic of oil volume in upper chamber is given by

$$\dot{\Upsilon}_i = h_i - \varepsilon_i(t) \tag{42}$$

where $\varepsilon_i(t)$ is the lumped reduction rate of oil attributed to consumption and other leakages. Likewise, the equation of motion of the poppet is

$$m_i\ddot{\Upsilon}_i = -k_i\dot{x}_i + T_i(t) + f_i \tag{43}$$

where m_i is the mass of the poppet, k_i is a viscous friction coefficient, and $T_i(t)$ is the lumped elastic force. Conduct the following notation substitution:

$$\chi_{i,1} = \Upsilon_i, \ \ \chi_{i,2} = x_i, \ \ \chi_{i,3} = \dot{x}_i, \ \ u_i = f_i. \tag{44}$$

Then, the dynamic of systems (42) and (43) comes down to

$$\begin{cases} \dot{\chi}_{i,1} = \phi_{i,1}\chi_{i,2}^3 + \psi_{i,1} \\ \dot{\chi}_{i,2} = \chi_{i,3} \\ \dot{\chi}_{i,3} = \phi_{i,3}u_i + \psi_{i,3} \end{cases} \tag{45}$$

where $\phi_{i,1} = \lambda_i\epsilon_i^3$, $\psi_{i,1} = -\varepsilon_i(t)$, $\phi_{i,3} = 1/m_i$, and $\psi_{i,3} = (1/m_i)[T_i(t) - k_i\chi_{i,3}]$ with $\lambda_1 = 2$ Mpa/Pa.s, $\lambda_2 = 2.2$ Mpa/Pa.s, $\lambda_3 = 2.15$ Mpa/Pa.s, $\lambda_4 = 2.3$ Mpa/Pa.s, $\varepsilon_1(t) = 0.25\chi_{1,1}$ lpm,

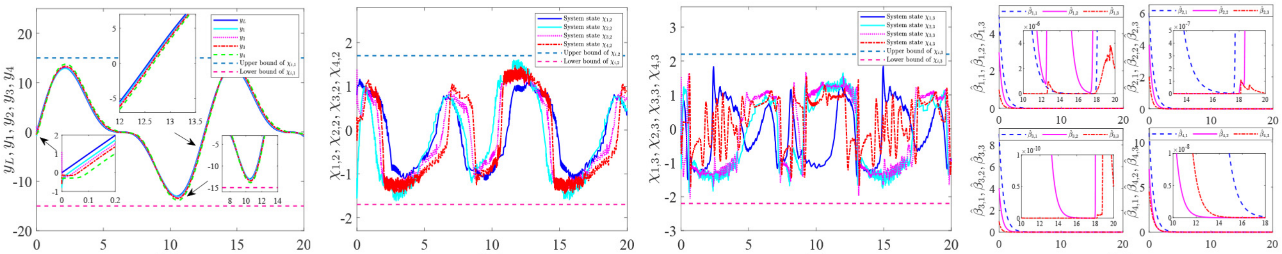

Fig. 2. Evolutions of (a) y_L, y_1, y_2, y_3, and y_4 of (b) agent dynamics states $\chi_{1,2}$, $\chi_{2,2}$, $\chi_{3,2}$, and $\chi_{4,2}$, (c) of agent dynamics states $\chi_{1,3}$, $\chi_{2,3}$, $\chi_{3,3}$, and $\chi_{4,3}$, (d) of parameter adaptive laws $\widehat{\beta}_{1,1}$, $\widehat{\beta}_{1,2}$, $\widehat{\beta}_{1,3}$, $\widehat{\beta}_{2,1}$, $\widehat{\beta}_{2,2}$, $\widehat{\beta}_{2,3}$, $\widehat{\beta}_{3,1}$, $\widehat{\beta}_{3,2}$, $\widehat{\beta}_{3,3}$, $\widehat{\beta}_{4,1}$, $\widehat{\beta}_{4,2}$, and $\widehat{\beta}_{4,3}$.

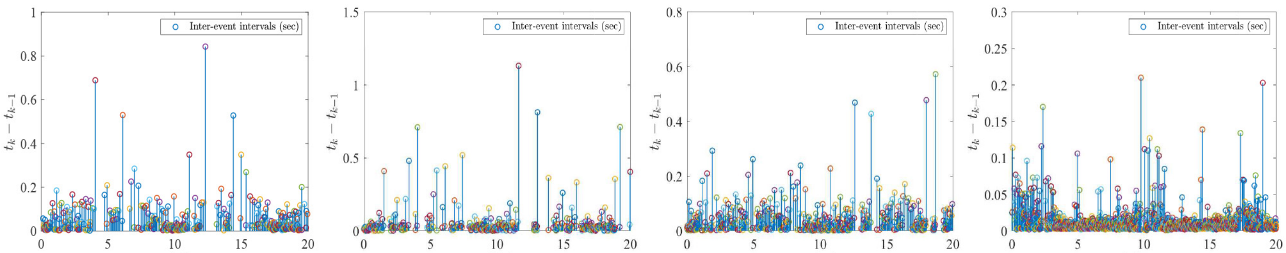

Fig. 3. Time intervals of triggering events (a) of follower agent 1, (b) of follower agent 2, (c) of follower agent 3, (d) of follower agent 4.

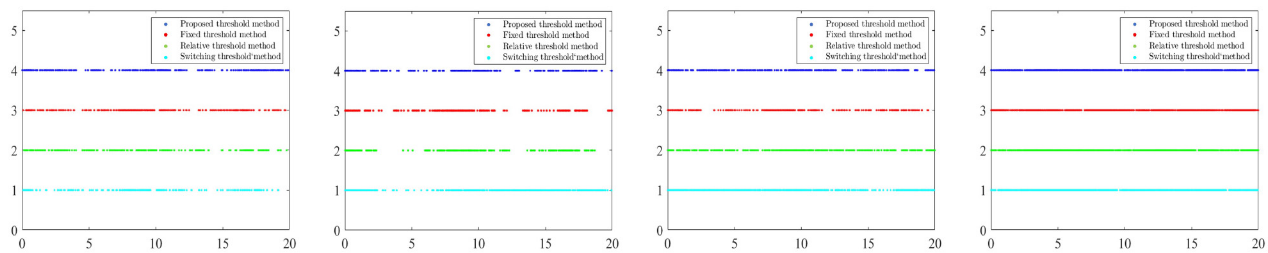

Fig. 4. Comparisons of triggering event (a) of agent 1, (b) of agent 2, (c) of agent 3, (d) of agent 4 between proposed method and existing methods.

$\varepsilon_2(t) = 1.2\chi_{2,1}$ lpm, $\varepsilon_3(t) = 1.5\chi_{3,1}$ lpm, $\varepsilon_4(t) = 1.1\chi_{4,1}$ lpm, $m_1 = 2.8$ kg, $m_2 = 2.95$ kg, $m_3 = 3$ kg, $m_4 = 2.9$ kg, $T_1(t) = 1.3\chi_{1,1}^3$ N, $T_2(t) = 1.8\chi_{2,1}^3$ N, $T_3(t) = 1.5\chi_{3,1}^3$ N, $T_4(t) = 2.4\chi_{4,1}^3$ N, $k_1 = 3.2$ N/mm, $k_2 = 3.25$ N/mm, $k_3 = 3.4$ N/mm, $k_4 = 3.35$ N/mm, $\epsilon_1 = 1.45$, $\epsilon_2 = 1.5$, $\epsilon_3 = 1.53$, $\epsilon_4 = 1.58$,. The simulation is run with the initial conditions $y_L(0) = 0$, $\boldsymbol{\chi}_1(0) = [-0.8, 0.8, -0.5]^T$, $\boldsymbol{\chi}_2(0) = [1.1, -1.1, 0.9]^T$, $\boldsymbol{\chi}_3(0) = [-0.6, 0.6, -0.4]^T$, and $\boldsymbol{\chi}_4(0) = [-0.3, 0.3, -0.2]^T$ and $\widehat{\beta}_{1,1}(0) = 5$, $\widehat{\beta}_{1,2}(0) = 3$, $\widehat{\beta}_{1,3}(0) = 1$, $\widehat{\beta}_{2,1}(0) = 6$, $\widehat{\beta}_{2,2}(0) = 4$, $\widehat{\beta}_{2,3}(0) = 2$, $\widehat{\beta}_{3,1}(0) = 9$, $\widehat{\beta}_{3,2}(0) = 4$, $\widehat{\beta}_{3,3}(0) = 1$, $\widehat{\beta}_{4,1}(0) = 11$, $\widehat{\beta}_{4,2}(0) = 7$, and $\widehat{\beta}_{4,3}(0) = 4.5$. Besides, the design parameters are chosen as $\omega_{1,1} = \omega_{1,2} = \omega_{1,3} = 2.6$, $\omega_{2,1} = \omega_{2,2} = \omega_{2,3} = 2.4$, $\omega_{3,1} = \omega_{3,2} = \omega_{3,3} = 3$, $\omega_{4,1} = \omega_{4,2} = \omega_{4,3} = 3.2$, $\Gamma_{1,1} = \Gamma_{1,2} = \Gamma_{1,3} = 0.75$, $\Gamma_{2,1} = \Gamma_{2,2} = \Gamma_{2,3} = 1$, $\Gamma_{3,1} = \Gamma_{3,2} = \Gamma_{3,3} = 1.1$, $\Gamma_{4,1} = \Gamma_{4,2} = \Gamma_{4,3} = 1.2$, $\xi_{1,1} = \xi_{1,2} = \xi_{1,3} = 0.65$, $\xi_{2,1} = \xi_{2,2} = \xi_{2,3} = 0.8$, $\xi_{3,1} = \xi_{3,2} = \xi_{3,3} = 1.1$, $\xi_{4,1} = \xi_{4,2} = \xi_{4,3} = 1.15$, $\gamma_{1,1} = \gamma_{1,2} = \gamma_{1,3} = 2.1$, $\gamma_{2,1} = \gamma_{2,2} = \gamma_{2,3} = 2.3$, $\gamma_{3,1} = \gamma_{3,2} = \gamma_{3,3} = 2.4$, and $\gamma_{4,1} = \gamma_{4,2} = \gamma_{4,3} = 2.5$, $\delta_{i,0} = 0.1$, $\delta_{i,1} = 0.8$, $\delta_{i,2} = 1.1$, $\lambda_{i,0} = 0.6$, $\tau_{i,0} = 0.8$, $\kappa_{i,0} = 0.7$, $\epsilon = 0.3$, and $\upsilon_{i,m} = 3$ for $i = 1, 2, 3, 4$ and $m = 1, 2, 3$. In addition, the upper bounds of agent dynamics states are confined as $k_{b_{i,1}} = 15$, $k_{b_{i,2}} = 1.8$, and $k_{b_{i,3}} = 2.2$. The simulation results are shown in Figs. 2–5.

Fig. 2(a) displays that all the follower agents can successfully track the reference signal with bounded consensus tracking errors, and the boundedness of agent dynamics states $\chi_{i,2}$, $\chi_{i,3}$, $i = 1, 2, 3, 4$ are shown in Figs. 2(b) and (c). It is clear from these figures that the full-state constraints are not violated. Fig. 2(d) provides the evolutions of $\widehat{\beta}_{1,1}$, $\widehat{\beta}_{2,1}$, $\widehat{\beta}_{3,1}$, and $\widehat{\beta}_{4,1}$, and of $\widehat{\beta}_{1,2}$, $\widehat{\beta}_{2,2}$, $\widehat{\beta}_{3,2}$, and $\widehat{\beta}_{4,2}$, and of $\widehat{\beta}_{1,3}$, $\widehat{\beta}_{2,3}$, $\widehat{\beta}_{3,3}$, and $\widehat{\beta}_{4,3}$, respectively. Fig. 3 reveals the time interval results of the triggering events. The event-triggered times and the threshold value comparisons of the proposed high-order event-triggered scheme and the other three event-triggered schemes in [24] are shown in Figs. 4 and 5, respectively. It can be observed that the proposed high-order ETC mechanism is feasible and it is more effective than the other three event-triggered schemes in [24].

In addition, the integral time absolute error (ITAE) $[\int_0^T t|s_{i,1}(t)|dt]$, root mean square error (RMSE) $[(1/T)\int_0^T s_{i,1}^2(t)dt]^{(1/2)}$, mean absolute error (MAE) $[(1/T)\int_0^T |s_{i,1}(t)|dt]$, and mean absolute control action (MACA) $[(1/T)\int_0^T |u_i|]$ are utilized here to quantify the

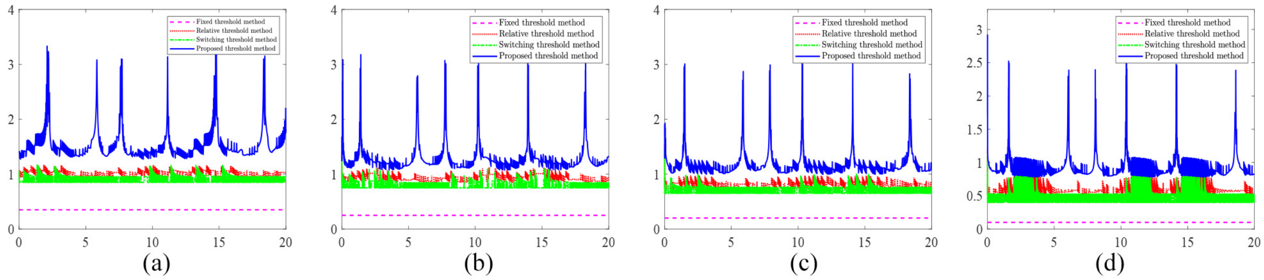

Fig. 5. Comparisons of threshold values (a) of agent 1, (b) of agent 2, (c) of agent 3, (d) of agent 4 between proposed method and existing methods.

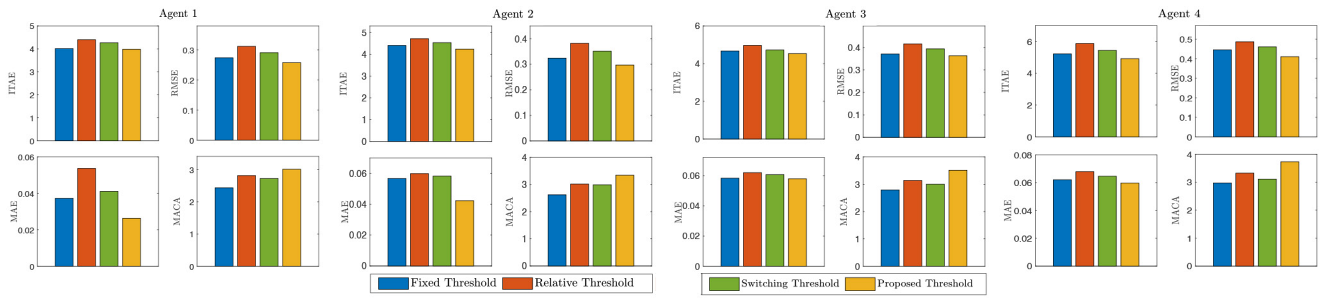

Fig. 6. Comparison of performance indexes between proposed method and existing methods.

TABLE I
PERFORMANCE INDICES FOR FOUR METHODS

Agent	Index	Fixed Threshold	Relative Threshold	Switching Threshold	Proposed Threshold	Agent	Index	Fixed Threshold	Relative Threshold	Switching Threshold	Proposed Threshold
Agent 1	ITAE	4.011	4.397	4.268	3.981	Agent 3	ITAE	4.671	4.964	4.723	4.533
	RMSE	0.274	0.312	0.291	0.258		RMSE	0.371	0.416	0.394	0.363
	MAE	0.0373	0.0537	0.0411	0.0263		MAE	0.0583	0.062	0.0607	0.0579
	MACA	2.436	2.816	2.727	3.012		MACA	2.793	3.141	3.004	3.516
	NUMBER	524	471	495	442		NUMBER	647	598	614	572
Agent 2	ITAE	4.402	4.716	4.532	4.237	Agent 4	ITAE	5.218	5.872	5.446	4.921
	RMSE	0.324	0.382	0.351	0.297		RMSE	0.446	0.487	0.461	0.411
	MAE	0.0567	0.0598	0.0582	0.0423		MAE	0.0621	0.0679	0.0646	0.0597
	MACA	2.619	3.016	2.989	3.343		MACA	2.974	3.326	3.112	3.734
	NUMBER	729	661	692	643		NUMBER	2780	2698	2724	2673

tracking performances of four different ETC schemes, respectively. More especially, Table I and Fig. 6 give the comparison results of the event-triggered numbers, ITAE, RMSE, MAE, and MACA of the four different event-triggering mechanisms. It can be seen from Table I and Fig. 6 that the proposed high-order event-triggering mechanism can give a larger threshold to trigger the events as less as possible, while making the consensus tracking errors smaller than other three event-triggering mechanisms.

VI. CONCLUSION

In this article, a novel event-triggered-constrained consensus tracking control methodology was proposed for high-order nonlinear multiagent networks with event-triggered input. To this purpose, a monotonically decreasing function was embedded into the design of the proposed high-order event-triggered mechanism so as to give a larger threshold to trigger the events as less as possible, while making the consensus tracking errors smaller. Comparative simulation results confirmed the superiority of the presented control scheme. An interesting problem to be investigated in the future is how to solve the distributed event-triggered consensus tracking problem for the high-order nonlinear multiagent networks with unknown control directions [45]. Besides, note that the event-triggered-constrained consensus tracking control of switched multiagent networks is an important but difficult issue, thus, the extension of our control scheme to the case of high-order switched multiagent networks will be another interesting topic for further investigation.

APPENDIX

Proof of Theorem 1 [Step $i, n_i (i = 1, \ldots, M)$]: Take the high-order tan-type BLF as

$$V_{i,n_i} = V_{i,n_i-1} + \frac{2k_{c_{i,n_i}}^{q_i-p_{i,n_i}+2}}{\pi\left(q_i - p_{i,n_i} + 2\right)} \tan\left(\frac{\pi s_{i,n_i}^{q_i-p_{i,n_i}+2}}{2k_{c_{i,n_i}}^{q_i-p_{i,n_i}+2}}\right) + \frac{1}{2\gamma_{i,n_i}}\tilde{\beta}_{i,n_i}^2 \tag{46}$$

where $k_{c_{i,n_i}} = k_{b_{i,n_i}} - \chi^*_{i,n_i,c}$ is an upper bound of s_{i,n_i} defined in a set $\Omega_{s_{i,n_i}} = \{s_{i,n_i} | |s_{i,n_i}| < k_{c_{i,n_i}}\}$ with $\chi^*_{i,n_i,c}$ being a constant specified later. $\widetilde{\beta}_{i,n_i} = \beta_{i,n_i} - \widehat{\beta}_{i,n_i}$ and $\gamma_{i,n_i} > 0$ is a design parameter. In view of (1), (4), and (46), the time derivative of V_{i,n_i} is

$$\begin{aligned}\dot{V}_{i,n_i} \le & \sum_{m=1}^{n_i-1} \Theta_{i,m} - \sum_{m=1}^{n_i} k_{i,m} \tan\left(\frac{\pi s_{i,m}^{q_i-p_{i,m}+2}}{2k_{c_{i,m}}^{q_i-p_{i,m}+2}}\right) - \frac{\widetilde{\beta}_{i,n_i}\dot{\widehat{\beta}}_{i,n_i}}{\gamma_{i,n_i}} \\ & + \sum_{m=1}^{n_i-1}\left(\frac{1}{2}\upsilon_{i,m}\left(\beta_{i,m}^2 - \widetilde{\beta}_{i,m}^2\right)\right) + s_{i,n_i}^{q_i+1}\overline{\vartheta}_{i,n_i-1} \\ & + \frac{s_{i,n_i}^{q_i-p_{i,n_i}+1}}{\Xi_{i,n_i}}\left(\phi_{i,n_i}(\boldsymbol{\chi}_i)u_i^{p_{i,n_i}} + \mathcal{F}_{i,n_i}(\mathbf{Z}_{i,n_i})\right) \\ & - \frac{s_{i,n_i}^{q_i-p_{i,n_i}+1}}{\Xi_{i,n_i}}\dot{\chi}_{i,n_i,c}^c - \frac{s_{i,n_i}^{q_i-p_{i,n_i}+1}}{\Xi_{i,n_i}}\varsigma_{i,n_i-1} \end{aligned} \tag{47}$$

where $\mathcal{F}_{i,n_i}(\mathbf{Z}_{i,n_i}) = \sin([\pi s_{i,n_i}^{q_i-p_{i,n_i}+2}]/[2k_{c_{i,n_i}}^{q_i-p_{i,n_i}+2}]) \cos([\pi s_{i,n_i}^{q_i-p_{i,n_i}+2}]/[2k_{c_{i,n_i}}^{q_i-p_{i,n_i}+2}])k_{i,n_i}s_{i,n_i}^{-(q_i-p_{i,n_i}+1)} + \psi_{i,n_i}(\boldsymbol{\chi}_i)$ and $\mathbf{Z}_{i,n_i} = [\boldsymbol{\chi}_i^T, \boldsymbol{\chi}_j^T, \widehat{\beta}_{i,1}, \widehat{\beta}_{i,2}, \ldots, \widehat{\beta}_{i,n_i-1}, y_L, \dot{y}_L, \ddot{y}_L]^T$. Along similar lines as step 1, it can be obtained that

$$\begin{aligned}\frac{s_{i,n_i}^{q_i-p_{i,n_i}+1}}{\Xi_{i,n_i}}\mathcal{F}_{i,n_i} = & \frac{s_{i,n_i}^{q_i-p_{i,n_i}+1}}{\Xi_{i,n_i}}\left(\boldsymbol{W}_{i,n_i}^{*T}\boldsymbol{S}_{i,n_i} + o_{i,n_i}\right) \\ \le & s_{i,n_i}^{q_i+1}\Xi_{i,n_i}^{-\bar{p}_{i,n_i}}\Gamma_{i,n_i}^{\bar{p}_{i,n_i}}\beta_{i,n_i}\Phi_{i,n_i}^{\bar{p}_{i,n_i}} + \omega_{i,n_i}^{-\underline{p}_{i,n_i}}\kappa_{i,n_i}^{\underline{p}_{i,n_i}} \\ & + s_{i,n_i}^{q_i+1}\Xi_{i,n_i}^{-\bar{p}_{i,n_i}}\omega_{i,n_i}^{\bar{p}_{i,n_i}} + \Gamma_{i,n_i}^{-\underline{p}_{i,n_i}} \end{aligned} \tag{48}$$

with $\|\boldsymbol{S}_{i,n_i}\| = \Phi_{i,n_i}$, $\beta_{i,n_i} = \|\boldsymbol{W}_{i,n_i}^*\|^{\bar{p}_{i,n_i}}$. Besides, using Lemma 3 yields $-s_{i,n_i}^{q_i-p_{i,n_i}+1}\Xi_{i,n_i}^{-1}\varsigma_{i,n_i-1} \le s_{i,n_i}^{q_i+1}\Xi_{i,n_i}^{-\bar{p}_{i,n_i}}\xi_{i,n_i}^{\bar{p}_{i,n_i}} + \xi_{i,n_i}^{-\underline{p}_{i,n_i}}\varsigma_{i,n_i-1}^{*\underline{p}_{i,n_i}}$, where $\Theta_{i,n_i} = \Gamma_{i,n_i}^{-\underline{p}_{i,n_i}} + \omega_{i,n_i}^{-\underline{p}_{i,n_i}}\kappa_{i,n_i}^{\underline{p}_{i,n_i}} + \xi_{i,n_i}^{-\underline{p}_{i,n_i}}\varsigma_{i,n_i-1}^{*\underline{p}_{i,n_i}}$ and $\underline{p}_{i,n_i} = ([q_i+1]/p_{i,n_i})$. The derivative of V_{i,n_i} along (47) and (48) is

$$\begin{aligned}\dot{V}_{i,n_i} \le & \sum_{m=1}^{n_i}\Theta_{i,m} + \frac{s_{i,n_i}^{q_i-p_{i,n_i}+1}}{\Xi_{i,n_i}}\left(\phi_{i,n_i}(\boldsymbol{\chi}_i)u_i^{p_{i,n_i}} - \dot{\chi}_{i,n_i,c}^c\right) \\ & + s_{i,n_i}^{q_i+1}\Xi_{i,n_i}^{-\bar{p}_{i,n_i}}\left(\omega_{i,n_i}^{\bar{p}_{i,n_i}} + \xi_{i,n_i}^{\bar{p}_{i,n_i}} + \Gamma_{i,n_i}^{\bar{p}_{i,n_i}}\beta_{i,n_i}\Phi_{i,n_i}^{\bar{p}_{i,n_i}}\right) \\ & - \sum_{m=1}^{n_i}k_{i,m}\tan\left(\frac{\pi s_{i,m}^{q_i-p_{i,m}+2}}{2k_{c_{i,m}}^{q_i-p_{i,m}+2}}\right) - \frac{\widetilde{\beta}_{i,n_i}\dot{\widehat{\beta}}_{i,n_i}}{\gamma_{i,n_i}} \\ & + \sum_{m=1}^{n_i-1}\left(\frac{1}{2}\upsilon_{i,m}\left(\beta_{i,m}^2 - \widetilde{\beta}_{i,m}^2\right)\right) + s_{i,n_i}^{q_i+1}\overline{\vartheta}_{i,n_i-1}. \end{aligned} \tag{49}$$

According to (38) and substituting (37) to (49), it can be obtained that $s_{i,n_i}\upsilon_i(t) \le 0$. Therefore, the following inequality holds:

$$\begin{aligned}\dot{V}_{i,n_i} \le & \sum_{m=1}^{n_i}\Theta_{i,m} - \sum_{m=1}^{n_i}k_{i,m}\tan\left(\frac{\pi s_{i,m}^{q_i-p_{i,m}+2}}{2k_{c_{i,m}}^{q_i-p_{i,m}+2}}\right) + s_{i,n_i}^{q_i+1}\overline{\vartheta}_{i,n_i-1} \\ & + \sum_{m=1}^{n_i-1}\left(\frac{1}{2}\upsilon_{i,m}\left(\beta_{i,m}^2 - \widetilde{\beta}_{i,m}^2\right)\right) - \frac{s_{i,n_i}^{q_i-p_{i,n_i}+1}}{\Xi_{i,n_i}}\dot{\chi}_{i,n_i,c}^c \\ & + s_{i,n_i}^{q_i+1}\Xi_{i,n_i}^{-\bar{p}_{i,n_i}}\left(\omega_{i,n_i}^{\bar{p}_{i,n_i}} + \xi_{i,n_i}^{\bar{p}_{i,n_i}} + \Gamma_{i,n_i}^{\bar{p}_{i,n_i}}\beta_{i,n_i}\Phi_{i,n_i}^{\bar{p}_{i,n_i}}\right) \\ & - \frac{\widetilde{\beta}_{i,n_i}\dot{\widehat{\beta}}_{i,n_i}}{\gamma_{i,n_i}} + \phi_{i,n_i}(\boldsymbol{\chi}_i) \\ & \times\left(\frac{s_{i,n_i}\Xi_{i,n_i}^{-\underline{q}_{i,n_i}}\upsilon_i(t)}{1+\delta_{i,0}} + \frac{\left|s_{i,n_i}\Xi_{i,n_i}^{-\underline{q}_{i,n_i}}\right|\left(\lambda_{i,0}s_{i,0} + \tau_{i,0}\right)}{1-\delta_{i,0}}\right)^{q_i-p_{i,n_i}+1} \end{aligned} \tag{50}$$

Substituting (38) into (50) and invoking Lemmas 1 and 2, (50) can be rewritten as

$$\begin{aligned}\dot{V}_{i,n_i} \le & s_{i,n_i}^{q_i+1}\Xi_{i,n_i}^{-\bar{p}_{i,n_i}}\left(\omega_{i,n_i}^{\bar{p}_{i,n_i}} + \xi_{i,n_i}^{\bar{p}_{i,n_i}} + \Gamma_{i,n_i}^{\bar{p}_{i,n_i}}\beta_{i,n_i}\Phi_{i,n_i}^{\bar{p}_{i,n_i}}\right) \\ & - \sum_{m=1}^{n_i}k_{i,m}\tan\left(\frac{\pi s_{i,m}^{q_i-p_{i,m}+2}}{2k_{c_{i,m}}^{q_i-p_{i,m}+2}}\right) + s_{i,n_i}^{q_i+1}\overline{\vartheta}_{i,n_i-1} \\ & - \frac{\widetilde{\beta}_{i,n_i}\dot{\widehat{\beta}}_{i,n_i}}{\gamma_{i,n_i}} + \phi_{i,n_i}(\boldsymbol{\chi}_i)r_{i,2}\left(0.557\delta_{i,1}\right)^{q_i-p_{i,n_i}+1} \\ & + \sum_{m=1}^{n_i}\Theta_{i,m} + \sum_{m=1}^{n_i-1}\left(\frac{1}{2}\upsilon_{i,m}\left(\beta_{i,m}^2 - \widetilde{\beta}_{i,m}^2\right)\right) \\ & + \phi_{i,n_i}(\boldsymbol{\chi}_i)r_{i,1}\left(s_{i,n_i}\Xi_{i,n_i}^{-\underline{q}_{i,n_i}}\alpha_{i,n_i}\right)^{q_i-p_{i,n_i}+1} \\ & - \frac{s_{i,n_i}^{q_i-p_{i,n_i}+1}}{\Xi_{i,n_i}}\dot{\chi}_{i,n_i,c}^c. \end{aligned} \tag{51}$$

Thus, the time derivative of V_{i,n_i} along (39)–(41) is

$$\begin{aligned}\dot{V}_{i,n_i} \le & -\sum_{m=1}^{n_i}k_{i,m}\tan\left(\frac{\pi s_{i,m}^{q_i-p_{i,m}+2}}{2k_{c_{i,m}}^{q_i-p_{i,m}+2}}\right) - \sum_{m=1}^{n_i}\frac{1}{2}\upsilon_{i,m}\widetilde{\beta}_{i,m}^2 \\ & + \sum_{m=1}^{n_i}\Theta_{i,m} + \phi_{i,n_i}(\boldsymbol{\chi}_i)r_{i,2}\left(0.557\delta_{i,1}\right)^{q_i-p_{i,n_i}+1} \\ & + \sum_{m=1}^{n_i}\frac{1}{2}\upsilon_{i,m}\beta_{i,m}^2. \end{aligned} \tag{52}$$

Consider the total high-order BLFs as

$$V = \sum_{i=1}^{M}\sum_{m=1}^{n_i}\left(\frac{2k_{c_{i,m}}^{q_i-p_{i,m}+2}}{\pi\left(q_i - p_{i,m} + 2\right)}\tan\left(\frac{\pi s_{i,m}^{q_i-p_{i,m}+2}}{2k_{c_{i,m}}^{q_i-p_{i,m}+2}}\right) + \frac{\widetilde{\beta}_{i,m}^2}{2\gamma_{i,m}}\right). \tag{53}$$

Then, (52) can be further expressed as

$$\dot{V}_{i,n_i} \le -\mu_i V_{i,n_i} + \eta_i \tag{54}$$

where $\mu_i = \min_{1\le m\le n_i}\{([k_{i,m}\pi(q_i - p_{i,m} + 2)]/[2k_{c_{i,m}}^{q_i-p_{i,m}+2}]), \gamma_{i,m}\upsilon_{i,m}\}$ and $\eta_i = \sum_{m=1}^{n_i}\Theta_{i,m} + \sum_{m=1}^{n_i}(1/2)\upsilon_{i,m}\beta_{i,m}^2 + \overline{\phi}_{i,n_i}\wp_{i,2}(0.557\delta_{i,1})^{q_i-p_{i,n_i}+1}$. Therefore, the derivative of V can be given by

$$\dot{V} \le -\alpha V + \varrho \tag{55}$$

where $\alpha = \min\{\mu_i, 1 \le i \le M\}$ and $\varrho = \sum_{i=1}^{M}\eta_i$. It can be concluded from (55) that $V(t)$ is eventually bounded by (ϱ/α), which can be made arbitrarily small by decreasing $\Gamma_{i,m}$, $\upsilon_{i,m}$, $\omega_{i,m}$, and $\xi_{i,m}$ and meanwhile increasing $\gamma_{i,m}$. Namely, it is possible to make $(\varrho/\alpha) \le \Pi$ by selecting the design parameters appropriately. Thus, given any initial condition satisfying $V(0) \leq \Pi$, we have $\dot{V}(t) \leq 0$ and $V(t) \leq \Pi$ for all $t \geq 0$. It follows that $V(t)$ is bounded. It can be deduced that $\tan([\pi s_{i,m}^{q_i-p_{i,m}+2}]/[2k_{c_{i,m}}^{q_i-p_{i,m}+2}])$ are also bounded. Consequently, the compact set $\Omega_{s_{i,m}} = \{s_{i,m}||s_{i,m}| < k_{c_{i,m}}\}$ is an invariant set and $s_{i,m}$ stays in the compact set $\Omega_{s_{i,m}}$ all the time.

Proposition 1: When $|s_{i,1}|$ is bounded, for any initial value $y_j(0) \geq 0$, there exists a known positive constant $y_{L,2}^*$ such that $|y_j(t)| \leq y_{L,2}^*$.

Proof: See the Appendix. ■

According to (4), we can obtain that $[\sum_{j\in\mathcal{N}_i} a_{ij} + \theta_i]|\chi_{i,1}| = |s_{i,1}| + \sum_{j\in\mathcal{N}_i} a_{ij}|y_j| + \theta_i|y_L|$. Based on (6) and the above analysis, it is clear that $|s_{i,1}| + \sum_{j\in\mathcal{N}_i} a_{ij}|y_j| + \theta_i|y_L| \leq k_{c_{i,1}} + \sum_{j\in\mathcal{N}_i} a_{ij}y_{L,1}^* + \theta_i y_L^* = [\sum_{j\in\mathcal{N}_i} a_{ij} + \theta_i]k_{b_{i,1}}$. Thus, the following inequality holds that $[\sum_{j\in\mathcal{N}_i} a_{ij} + \theta_i]|\chi_{i,1}| \leq [\sum_{j\in\mathcal{N}_i} a_{ij} + \theta_i]k_{b_{i,1}}$ and $|\chi_{i,1}| \leq k_{b_{i,1}}$. Since $\boldsymbol{\chi}_i$, $\boldsymbol{\chi}_j$, y_L, $\dot{y}_L$, $\ddot{y}_L$, and $\hat{\beta}_{i,1}$ are bounded and $\chi_{i,2,c}$ is continuous, it can be concluded that $\chi_{i,2,c}$ is bounded. Hence, there exists a positive constant $\chi_{i,2,c}^*$ such that $|\chi_{i,2,c}| \leq \chi_{i,2,c}^*$. According to (4) and it can be obtained that $|\chi_{i,2}| = |s_{i,2}| + |\chi_{i,2,c}| \leq k_{c_{i,2}} + \chi_{i,2,c}^* = k_{b_{i,2}}$ and $|\chi_{i,2}| \leq k_{b_{i,2}}$. Taking the same manipulations, it can be proved that $|\chi_{i,m}| \leq k_{b_{i,m}}$. Therefore, all the system states $\chi_{i,1}, \chi_{i,2}, \ldots, \chi_{i,n_i}$ are bounded and confined in the corresponding sets $\Omega_{\chi_{i,m}} := \{\chi_{i,m}||\chi_{i,m}| \leq k_{b_{i,m}}\}$. Therefore, property (1) of Theorem 1 is proved.

By (54) together with the fact $([\pi s_{i,1}^{q_i-p_{i,1}+2}]/[2k_{c_{i,1}}^{q_i-p_{i,1}+2}]) \leq \tan[(\pi s_{i,1}^{q_i-p_{i,1}+2})/(2k_{c_{i,1}}^{q_i-p_{i,1}+2})]$, it holds that

$$\frac{s_{i,1}^{q_i-p_{i,1}+2}}{q_i - p_{i,1} + 2} \leq V_{i,n_i}(0)e^{-\mu_i t} + \frac{\eta_i}{\mu_i}. \tag{56}$$

Noting (56), we know that $\lim_{t\to\infty} V_i(t) \leq (\eta_i/\mu_i)$, which leads to $\lim_{t\to\infty}|s_{i,1}| \leq ([\eta_i/\mu_i](q_i - p_{i,1} + 2))^{(1/[q_i-p_{i,1}+2])}$. Then, we can obtain

$$\lim_{t\to\infty}\|\boldsymbol{s}_1\| \leq \sqrt{\sum_{i=1}^{M}\lim_{t\to\infty}|s_{i,1}|^2} \leq \sqrt{\sum_{i=1}^{M}\Lambda^2} \tag{57}$$

where $\Lambda = ([\eta_i/\mu_i](q_i - p_{i,1} + 2))^{[1/(q_i-p_{i,1}+2)]}$. According to (57), we can obtain that $\lim_{t\to\infty}\|\boldsymbol{\delta}\| \leq (1/[\underline{\sigma}(\mathcal{L} + \mathcal{B})])\sqrt{\sum_{i=1}^{M}\Lambda^2}$ and property (2) of Theorem 1 is proved.

To prove the absence of Zeno-behavior, a time constant $T^* > 0$ can be found to satisfy $\{t_{h+1} - t_h\} \geq T^*$ $\forall h \in N^+$. By invoking $e_i(t) = \upsilon_i(t) - u_i^{\bar{q}_{i,n_i}}(t)$ and taking the time derivative of $e_i(t)$ for all $t \in [t_h, t_{h+1})$, we can get

$$\frac{d}{dt}|e_i| = \frac{d}{dt}\left(e_i^2\right)^{\frac{1}{2}} = \text{sign}(e_i)\dot{e}_i \leq |\dot{\upsilon}_i|. \tag{58}$$

Noting the expression of $\upsilon_i(t)$ in (38), we know that $\upsilon_i(t)$ is differentiable and $\dot{\upsilon}_i$ is a function of bounded variables, i.e., bounded signals of the multiagent networks. Therefore, there exists a constant $V_i^* > 0$ such that $|\dot{\upsilon}_i| \leq V_i^*$. Since $e_i(t_h) = 0$ and $\lim_{t\to t_{h+1}} e_i(t) = \delta_{i,0}|u_i^{\bar{q}_{i,n_i}}(t_{h+1})| + \lambda_{i,0}s_{i,0}(t_{h+1}) + \tau_{i,0}$, it can be obtained that the lower bound of interevent intervals T_i^* satisfies $T_i^* \geq ([\delta_{i,0}|u_i^{\bar{q}_{i,n_i}}(t_{h+1})| + \lambda_{i,0}s_{i,0}(t_{h+1}) + \tau_{i,0}]/V_i^*) \geq (\tau_{i,0}/V_i^*)$, which implies the Zeno behavior is effectively avoided. The proof is thus completed. ■

Proof of Proposition 1: The main idea is to prove the boundedness of $|y_j(t)|$ through seeking a contradiction. Noting (4), it can be obtained that $|s_{i,1}| = [\sum_{j\in\mathcal{N}_i} a_{ij} + \theta_i]|y_i| - \sum_{j\in\mathcal{N}_i} a_{ij}|y_j| - \theta_i|y_L|$. When $|s_{i,1}| < k_{c_{i,1}}$, we can obtain

$$\left(\sum_{j\in\mathcal{N}_i} a_{ij} + \theta_i\right)|y_i| - \sum_{j\in\mathcal{N}_i} a_{ij}|y_j| - \theta_i y_L^* < k_{c_{i,1}}. \tag{59}$$

At this point, four situations should be taken into account.

Situation I: Assuming that $|y_i|$ is unbounded as $|y_i| \to \infty$, $|y_j|$ is unbounded as $|y_j| \to \infty$.

Apparently, the terms on the left-hand side of (59) approach to infinity as $[\sum_{j\in\mathcal{N}_i} a_{ij} + \theta_i]|y_i| - \sum_{j\in\mathcal{N}_i} a_{ij}|y_j| - \theta_i y_L^* \to \infty$, which leads to a contradiction with the fact that $|s_{i,1}|$ is bounded.

Situation II: Assuming that $|y_i|$ is unbounded as $|y_i| \to \infty$, $|y_j|$ is bounded which satisfy $|y_j| \leq y_{L,2}^*$ with $y_{L,2}^*$ being known constant.

The proof is similar to Situation 1. When $|y_i| \to \infty$, $|y_j| \leq y_{L,2}^*$, the terms on the left hand of (59) approach to infinity as $[\sum_{j\in\mathcal{N}_i} a_{ij} + \theta_i]|y_i| - \sum_{j\in\mathcal{N}_i} a_{ij}y_{L,2}^* - \theta_i y_L^* \to \infty$, which leads to a contradiction with the fact that $|s_{i,1}|$ is bounded.

Situation III: Assuming that $|y_i|$ is bounded, $|y_j|$ is unbounded as $|y_j| \to \infty$.

Similarly, when $|y_i|$ is bounded, $|y_j| \to \infty$, the terms on the left hand of (59) approach to infinity as $[\sum_{j\in\mathcal{N}_i} a_{ij} + \theta_i]|y_i| - \sum_{j\in\mathcal{N}_i} a_{ij}y_{L,2}^* - \theta_i y_L^* \to \infty$, which leads to a contradiction with the fact that $|s_{i,1}|$ is bounded.

Situation IV: Assuming that $|y_i|$ is bounded, $|y_j|$ is bounded that satisfies $|y_j| \leq y_{L,2}^*$ with $y_{L,2}^*$ being known constant.

When $|y_i|$ is bounded, $|y_j|$ is bounded, the inequality $[\sum_{j\in\mathcal{N}_i} a_{ij} + \theta_i]|y_i| - \sum_{j\in\mathcal{N}_i} a_{ij}y_{L,2}^* - \theta_i y_L^* < k_{c_{i,1}}$ holds on, which means that there must exist a known positive constant $y_{L,2}^*$ such that $|y_j| \leq y_{L,2}^*$. Thus, the proof is thus completed. ■

References

[1] S. E. Ferik, H. A. Hashim, and F. L. Lewis, "Neuro-adaptive distributed control with prescribed performance for the synchronization of unknown nonlinear networked systems," *IEEE Trans. Syst., Man, Cybern., Syst.*, vol. 48, no. 12, pp. 2135–2144, Dec. 2018.

[2] I. Katsoukis and G. A. Rovithakis, "A low complexity robust output synchronization protocol with prescribed performance for high-order heterogeneous uncertain MIMO nonlinear multi-agent systems," *IEEE Trans. Autom. Control*, early access, Jul. 14, 2021, doi: 10.1109/TAC.2021.3096803.

[3] Y. Zhang, D. Wang, Z. Peng, and T. Li, "Distributed containment maneuvering of uncertain multiagent systems in MIMO strict-feedback form," *IEEE Trans. Syst., Man, Cybern., Syst.*, vol. 51, no. 2, pp. 1354–1364, Feb. 2021.

[4] J. Zhou, Y. Lv, G. Wen, and G. Chen, "Terminal-time synchronization of multi-vehicle systems under sampled-data communications," *IEEE Trans. Syst., Man, Cybern., Syst.*, early access, Jan. 25, 2021, doi: 10.1109/TSMC.2021.3049545.

[5] M. Meng, L. Liu, and G. Feng, "Adaptive output regulation of heterogeneous multiagent systems under Markovian switching topologies," *IEEE Trans. Cybern.*, vol. 48, no. 10, pp. 2962–2971, Oct. 2018.

[6] X. Guo, H. Ma, H. Liang, and H. Zhang, "Command-filter-based fixed-time bipartite containment control for a class of stochastic multiagent systems," *IEEE Trans. Syst., Man, Cybern., Syst.*, early access, Apr. 23, 2021, doi: 10.1109/TSMC.2021.3072650.

[7] M. Krstic, I. Kanellakopoulos, and P. Kokotovic, *Nonlinear and Adaptive Control Design*. New York, NY, USA: Wiley, 1995.

[8] H. Du, G. Wen, G. Chen, J. Cao, and F. E. Alsaadi, "A distributed finite-time consensus algorithm for higher-order leaderless and leader-following multiagent systems," *IEEE Trans. Syst., Man, Cybern., Syst.*, vol. 47, no. 7, pp. 1625–1634, Jul. 2017.

[9] Q. Zhou, W. Wang, H. Liang, M. V. Basin, and B. Wang, "Observer-based event-triggered fuzzy adaptive bipartite containment control of multi-agent systems with input quantization," *IEEE Trans. Fuzzy Syst.*, vol. 29, no. 2, pp. 372–384, Feb. 2021, doi: 10.1109/TFUZZ.2019.2953573.

[10] G. Wen, P. Wang, T. Huang, W. Yu, and J. Sun, "Robust neuro-adaptive containment of multileader multiagent systems with uncertain dynamics," *IEEE Trans. Syst., Man, Cybern., Syst.*, vol. 49, no. 2, pp. 406–417, Feb. 2019.

[11] W. Meng, P. X. Liu, Q. Yang, and Y. Sun, "Distributed synchronization control of nonaffine multiagent systems with guaranteed performance," *IEEE Trans. Neural Netw. Learn. Syst.*, vol. 31, no. 5, pp. 1571–1580, May 2020.

[12] N. Wang, Y. Wang, J. H. Park, M. Lv, and F. Zhang, "Fuzzy adaptive finite-time consensus tracking control of high-order nonlinear multi-agent networks with dead zone," *Nonlinear Dyn.*, early access, Nov. 1, 2021, doi: 10.1007/s11071-021-06956-5.

[13] C. J. Qian and W. Lin, "Output feedback control of a class of nonlinear systems: A nonseparation principle paradigm," *IEEE Trans. Autom. Control*, vol. 47, no. 10, pp. 1710–1715, Oct. 2002.

[14] Z. Sun, C.-Y. Liu, S.-F. Su, and W. Sun, "Robust stabilization of high-order nonlinear systems with unknown sensitivities and applications in humanoid robot manipulation," *IEEE Trans. Syst., Man, Cybern., Syst.*, vol. 51, no. 7, pp. 4409–4416, Jul. 2021.

[15] C. J. Qian and W. Lin, "Practical output tracking of nonlinear systems with uncontrollable unstable linearization," *IEEE Trans. Autom. Control*, vol. 47, no. 1, pp. 21–36, Jan. 2002.

[16] W. Lin and C. J. Qian, "Adding one power integrator: A tool for global stabilization of high-order lower-triangular systems," *Syst. Control Lett.*, vol. 39, no. 5, pp. 339–351, Apr. 2000.

[17] Z. Sun and Y. Liu, "Adaptive state-feedback stabilization for a class of high-order nonlinear uncertain systems," *Automatica*, vol. 43, pp. 1772–1783, Oct. 2007.

[18] X. Zhao, P. Shi, X. Zheng, and J. Zhang, "Intelligent tracking control for a class of uncertain high-order nonlinear systems," *IEEE Trans. Neural Netw. Learn. Syst.*, vol. 27, no. 9, pp. 1976–1982, Sep. 2016.

[19] X. Wang, H. Li, G. Zong, and X. Zhao, "Adaptive fuzzy tracking control for a calss of high-order switched uncertain nonlinear systems," *J. Franklin Inst.*, vol. 354, no. 4, pp. 6567–6587, 2017.

[20] M. Lv, W. Yu, J. Cao, and S. Baldi, "A separation-based methodology to consensus tracking of switched high-order nonlinear multi-agent systems," *IEEE Trans. Neural Netw. Learn. Syst.*, early access, Apr. 14, 2021, doi: 10.1109/TNNLS.2021.3070824.

[21] N. Wang, G. Wen, Y. Wang, F. Zhang, and A. Zemouche, "Fuzzy adaptive cooperative consensus tracking of high-order nonlinear multi-agent networks with guaranteed performances," *IEEE Trans. Cybern.*, early access, Feb. 26, 2021, doi: 10.1109/TCYB.2021.3051002.

[22] M. Lv, W. Yu, J. Cao, and S. Baldi, "Consensus in high-power multiagent systems with mixed unknown control directions via hybrid Nussbaum-based control," *IEEE Trans. Cybern.*, early access, Nov. 4, 2020, doi: 10.1109/TCYB.2020.3028171.

[23] L. Xing, C. Wen, Z. Liu, H. Su, and J. Cai, "Event-triggered output feedback control for a class of uncertain nonlinear systems," *IEEE Trans. Autom. Control*, vol. 64, no. 1, pp. 290–297, Jan. 2019.

[24] L. Xing, C. Wen, Z. Liu, H. Su, and J. Cai, "Event-triggered adaptive control for a class of uncertain nonlinear systems," *IEEE Trans. Autom. Control*, vol. 62, no. 4, pp. 2071–2076, Apr. 2017.

[25] L. Cao, H. Ren, H. Li, and R. Lu, "Event-triggered output-feedback control for large-scale systems with unknown hysteresis," *IEEE Trans. Cybern.*, vol. 51, no. 11, pp. 5236–5247, Nov. 2021, doi: 10.1109/TCYB.2020.2997943.

[26] Y.-X. Li and G.-H. Yang, "Model-based adaptive event-triggered control of strict-feedback nonlinear systems," *IEEE Trans. Neural Netw. Learn. Syst.*, vol. 29, no. 4, pp. 1033–1045, Apr. 2018.

[27] H. Ma, H. Li, H. Liang, and G. Dong, "Adaptive fuzzy event-triggered control for stochastic nonlinear systems with full state constraints and actuator faults," *IEEE Trans. Fuzzy Syst.*, vol. 27, no. 11, pp. 2242–2254, Nov. 2019.

[28] D. Yao, H. Li, R. Lu, and Y. Shi, "Event-triggered guaranteed cost leader-following consensus control of second-order nonlinear multiagent systems," *IEEE Trans. Syst., Man, Cybern., Syst.*, early access, Feb. 3, 2021, doi: 10.1109/TSMC.2021.3051346.

[29] W. Wang, S. Tong, and D. Wang, "Distributed sliding-mode tracking control of second-order nonlinear multiagent systems: An event-triggered approach," *IEEE Trans. Cybern.*, vol. 49, no. 3, pp. 961–973, Mar. 2019.

[30] Y. Zhang, H. Li, J. Sun, ang W. He, "Cooperative adaptive event-triggered control for multiagent systems with actuator failures," *IEEE Trans. Syst., Man, Cybern., Syst.*, vol. 49, no. 9, pp. 1759–1768, Sep. 2019.

[31] W. Wang, Y. Li, and S. Tong, "Adaptive fuzzy event-triggered control for leader-following consensus of high-order nonlinear systems," *IEEE Trans. Fuzzy Syst.*, vol. 28, no. 10, pp. 2389–2400, Oct. 2020, doi: 10.1109/TFUZZ.2019.2936359.

[32] L. N. Tan, "Event-triggered distributed $\mathcal{H}_\infty$ constrained control of physically interconnected large-scale partially unknown strict-feedback systems," *IEEE Trans. Syst., Man, Cybern., Syst.*, vol. 51, no. 4, pp. 2444–2456, Apr. 2021.

[33] Y. Liu, "Adaptive control-based barrier Lyapunov functions for a class of stochastic nonlinear systems with full state constraints," *Automatica*, vol. 87, pp. 83–93, Jan. 2018.

[34] M. Lv, Y. Li, W. Pan, and S. Baldi, "Finite-time fuzzy adaptive constrained tracking control for hypersonic flight vehicles with singularity-free switching," *IEEE/ASME Trans. Mechatronics*, early access, Jun. 18, 2021, doi: 10.1109/TMECH.2021.3090509.

[35] K. P. Tee and S. S. Ge, "Barrier Lyapunov functions for the control of output-constrained nonlinear systems," *Automatica*, vol. 45, pp. 918–927, Apr. 2009.

[36] Y. Liu, H. Zhang, J. Sun, and Y. Wang, "Adaptive fuzzy containment control for multi-agent systems with state constraints using unified transformation functions," *IEEE Trans. Fuzzy Syst.*, early access, Oct. 23, 2020, doi: 10.1109/TFUZZ.2020.3033376.

[37] Z. Liu and Z. Chen, "Discarded consensus of network of agents with state constraint," *IEEE Trans. Autom. Control*, vol. 57, no. 11, pp. 2869–2872, Nov. 2012.

[38] W. Wang and S. Tong, "Adaptive fuzzy containment control of nonlinear strict-feedback systems with full state constraints," *IEEE Trans. Fuzzy Syst.*, vol. 27, no. 10, pp. 2024–2038, Oct. 2019.

[39] W. Meng, Q. Yang, J. Si, and Y. Sun, "Consensus control of nonlinear multiagent systems with time-varying state constraints," *IEEE Trans. Cybern.*, vol. 47, no. 8, pp. 2110–2120, Aug. 2017.

[40] W. Sun, S. Su, G. Dong, and W. Bai, "Reduced adaptive fuzzy tracking control for high-order stochastic nonstrict feedback nonlinear system with full-state constraints," *IEEE Trans. Syst., Man, Cybern., Syst.*, vol. 51, no. 3, pp. 1496–1506, Mar. 2021.

[41] Y. Wu and X. Xie, "Adaptive fuzzy control for high-order nonlinear time-delay systems with full-state constraints and input saturation," *IEEE Trans. Fuzzy Syst.*, vol. 28, no. 8, pp. 1652–1663, Aug. 2020.

[42] L. X. Wang, "Stable adaptive fuzzy control of nonlinear systems," *IEEE Trans. Fuzzy Syst.*, vol. 1, no. 2, pp. 146–155, May 1993.

[43] S. S. Ge, C. Hang, and T. Zhang, "Stable adaptive control for nonlinear multivariable systems with a triangular control structure," *IEEE Trans. Autom. Control*, vol. 45, no. 6, pp. 1221–1225, Jun. 2000.

[44] N. D. Manring and R. C. Fales, *Hydraulic Control Systems*. New York, NY, USA: Wiley, 2020.

[45] M. Lv, B. De Schutter, C. Shi, and S. Baldi, "Logic-based distributed switching control for agents in power chained form with multiple unknown control directions," *Automatica*, to be published.

Ning Wang was born in Shanxi, China, in 1994. He received the B.S. degree in safety engineering from Air Force Engineering University, Xi'an, China, in 2017, where he is currently pursuing the Ph.D. degree in control science and engineering with the Air Traffic Control and Navigation College, Air Force Engineering University, Xi'an.

His research interests include nonlinear control, adaptive control, and multiagent networks.

Ying Wang received the B.S. degree in system science from the University of Science and Technology of China, Hefei, China, in 1990, and the M.S. and Ph.D. degrees from Xi'an Jiaotong University, Xi'an, China, in 1995 and 2002, respectively.

She is currently a Professor with the Air Traffic Control and Navigation College, Air Force Engineering University, Xi'an. Her research interests include adaptive control, backstepping control, multiagent networks, and airspace management.

Guanghui Wen (Senior Member, IEEE) received the Ph.D. degree in mechanical systems and control from Peking University, Beijing, China, in 2012.

He is currently a Professor with the Department of Systems Science, School of Mathematics, Southeast University, Nanjing, China. His current research interests include autonomous intelligent systems, complex networked systems, distributed control and optimization, resilient control, and distributed reinforcement learning.

Prof. Wen was a recipient of the Best Student Paper Award in the 6th Chinese Conference on Complex Networks in 2010, the Australian Research Council Discovery Early Career Researcher Award in 2018, and the Asia Pacific Neural Network Society Young Researcher Award in 2019. He was awarded the National Natural Science Fund for Excellent Young Scholars in 2017. He has been named a Highly Cited Researcher by Clarivate Analytics since 2018. He is a Reviewer for *American Mathematical Review* and an active reviewer for many journals. He currently serves as an Associate Editor of the IEEE JOURNAL OF EMERGING AND SELECTED TOPICS IN INDUSTRIAL ELECTRONICS, the IEEE TRANSACTIONS ON SYSTEMS, MAN AND CYBERNETICS: SYSTEMS, the IEEE Open Journal of the Industrial Electronics Society, and the *Asian Journal of Control*.

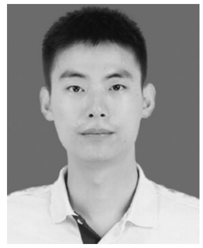

Maolong Lv received the B.S. degree in electrical engineering and automation and M.S. degree in control science and engineering from Air Force Engineering University, Xi'an, China, in 2014 and 2016, respectively, and the Ph.D. degree from the Delft Center for Systems and Control, Delft University of Technology, Delft, The Netherlands, in 2021.

He is currently with the College of Air Traffic Control and Navigation, Air Force Engineering University, Xi'an. His research interests include adaptive learning control, deep reinforcement learning, distributed control, and intelligent decision with applications in multiagent systems, hypersonic flight vehicles, and unmanned autonomous system.

Dr. Lv was awarded the Descartes Excellence Fellowship from the French Government in 2018, which allowed him a research visit and a cooperation with the University of Grenoble on the topic of adaptive networked systems with emphasis on ring stability analysis for mixed traffic with human driven and autonomous vehicles from 2018 to 2019.

Fan Zhang received the B.S. degree in automation and the M.S. degree in flight vehicle design from the Harbin Institute of Technology, Harbin, China, in 2008 and 2010, respectively, and the Ph.D. degree in systems and control from the University of Groningen, Groningen, The Netherlands, in 2015.

He is currently an Associate Professor with the School of Aeronautics and Astronautics (Shenzhen Campus), Sun Yat-sen University, Guangzhou, China. His research interests include estimation, control, and learning in cyber–physical systems and multiagent networks.